AD-A131 796 INFRARED CHARACTERISTICS OF GAS PLUMES(U) SOUTH AUSTRALIAN INST OF TECH ADELAIDE SCHOOL OF CHEMICAL TECHNOLOGY A STEVEN ET AL. AUG 82 82-2 1/1

UNCLASSIFIED F/G 21/2 NL

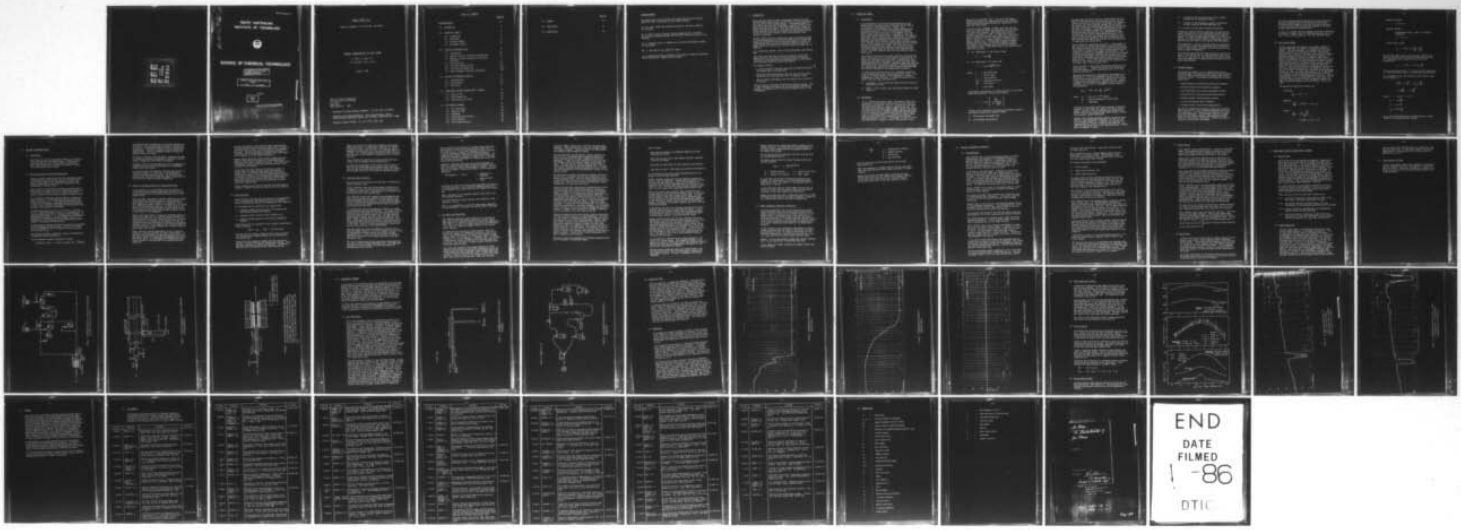

END
DATE FILMED
1-86
DTIC

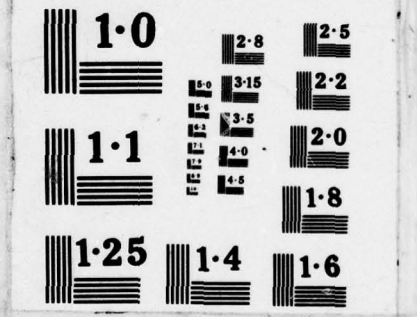
1·0
1·1
1·25
2·8
3·15
3·5
4·0
4·5
1·4
2·5
2·2
2·0
1·8
1·6

SOUTH AUSTRALIAN INSTITUTE OF TECHNOLOGY

SCHOOL OF CHEMICAL TECHNOLOGY

INFRARED CHARACTERISTICS OF GAS PLUMES

A. STEVEN, G.T. WILKINSON.

#82-2.

AUGUST
1982

This document has been approved for public release and sale; its distribution is unlimited.

ANNUAL REPORT 82-2

Research Agreement: DST 431/1/328, CDS 268/81

INFRARED CHARACTERISTICS OF GAS PLUMES

A. Steven (B. App. Sci.)

G.T. Wilkinson (B.E., Ph.D.)

August, 1982.

School of Chemical Technology,
S.A. Institute of Technology,
P.O. Box 1,
Ingle Farm,
South Australia, 5098.

- Department of Defence Research Agreement: DST 431/1/328, CDS 268/81.

- Department Co-ordinating Authority: Chief Superintendent, Weapons Systems Research Laboratory (WSRL), DRC, Salisbury, South Australia. 5108

- Department Contact Officer: Dr. W.H. Jolley, WSRL, DRCS.

TABLE OF CONTENTS

		Page No.
ACKNOWLEDGEMENTS		4
1.0	INTRODUCTION	5
2.0	THEORETICAL MODELS	6
2.1	Introduction	6
2.2	Band Models	6
2.3	Scattering Models	9
2.4	Gas Dynamic Models	10
3.0	PREVIOUS EXPERIMENTAL WORK	12
3.1	Introduction	12
3.2	Species Involved, IR Emission and Reactions	12
3.3	Effect on Infrared Radiation of Aluminium Particles	13
3.4	Other Particles	14
3.5	Size Distribution of Al_2O_3	15
3.6	O/F Ratio and Choked Flow	16
3.7	Other Parameters Effecting IR Radiation	19
4.0	PREVIOUS EXPERIMENTAL APPARATUS	21
4.1	Instrumentation	21
4.2	Burner Design	23
4.3	Ancillaries	23
5.0	AREAS WHERE FURTHER RESEARCH WORK IS NEEDED	24
5.1	Particle Size	24
5.2	Plume Composition	24
5.3	Flow Structure of Plume	25
6.0	EXPERIMENTAL PROGRAM	29
6.1	Gas Flame Burner	29
6.2	Combustion Tube	32
6.3	Radiometer	32
6.4	Flame Temperature Profile	36
6.5	Profile Results	36
6.6	Solids Sampling Probe	36

		Page No.
7.0	SUMMARY	40
8.0	BIBLIOGRAPHY	41
9.0	NOMENCLATURE	48

ACKNOWLEDGEMENTS

The authors would like to express their appreciation to the following people for their contribution to this research program.

Dr. R.M. Lough, (DRCS) who provided assistance in the early stages of this program.

Dr. W. Jolley, Propulsion Group, Defence Research Centre, Salisbury, who provided invaluable guidance and assistance during the course of this research.

Mr. P. Stimburys and Mr. S. Sweeney who assisted with equipment assembly and procurement.

Mrs. R. Jones who so ably typed this report.

Dr. N. Cheetham and other colleagues in the School of Chemical Technology, who provided helpful comments and assistance.

1.0 INTRODUCTION

During the past decade or more, considerable attention has been directed towards the character and intensity of infra-red emissions from missile and other exhaust plumes. A considerable amount of experimental data has been accumulated on several systems such as those involving liquid and solid fueled rocket motors, turbo jet engines and turbulent flames. This data has been incorporated to varying degrees in several plume modelling programs which evolved in the '70's and have reached a level giving reliable plume character prediction.

The main reasons for this interest have been to advance knowledge of infra-red technology for the better prediction of radiant heat energy and temperature fields from rocket exhausts to launch pad installations, and as an aid in designing effective infra-red seeker systems for anti-aircraft and anti-missile missiles and for spoofing.

It is recognised, however, that existing plume models need improvement.

This report describes the results of a research program undertaken at the S.A. Institute of Technology, School of Chemical Technology to study the infra-red characteristics of high temperature gas plumes containing particulate material.

The program involved:-

- a critical survey of the open literature and identification of significant gaps in the data base,
- the design and construction of a hot gas test rig for investigating the infra-red characteristics of turbulent flames,
- and preliminary experimental work to establish the reliability of the rig.

The first part of the report contains the literature review. This is then followed by the results of the preliminary experimental program. A complete list of literature surveyed is given in the bibliography.

2.0 THEORETICAL MODELS

2.1 Introduction

An understanding of the infra-red characteristics of gas plumes implies an appreciation of both emission and absorption spectra of the plume species. Strong core emissions will be attenuated by the cooler absorbing gases surrounding the plume. Thus both black-body and species emitters (molecular, ions, etc.) in the exhaust will have their radiant intensity modified in character by their own enveloping cloud of exhaust gases. Furthermore, in situations where high velocity exhaust species interact with the ambient atmosphere the energy transfer can give rise to plasma emissions which now originate in areas remote from the exhaust core. Rocket exhausts are characteristically fuel-rich and can generate long afterburning plumes. This flame can be distinguished from the primary combustion zone occuring within the rocket chamber where most of the fuel-oxidant reaction occurs. This work concerns itself with the external flame or plume stage.

The problem of describing the highly turbulent, sometimes two-phase, flow which exists in rocket exhaust flames combines the specialist knowledge of several fields: compressible, high temperature two-phase flow dynamics in which solid and liquid condensed phases may be present; combustion chemistry involving fast kinetics and free radicle reactions; emission and absorption spectroscopy, particularly that related to the infra-red; and numerical mathematics and computational procedures.

In examining the plume structure it is customary to measure axial distances down stream from the nozzle exit plane. Axial symmetry is assumed leading to two-dimensional or pseudo-unidimensional simplifications. In examining existing plume models, they have been subdivided into

a) Band models: used to describe specifically the infra-red characteristics, and

b) Others: which includes other significant aspects of plume modeling.

2.2 Band Models

If in a specific wavelength region, the physical state of an absorbing or emitting gas is known as well as the locations, intensities and shapes of lines, it is possible to calculate the radiation emitted by a specific sample of the gas. For the gases associated with exhaust plumes, however, the absorption coefficient varies extremely rapidly with wavelength and an exact calculation of radiant heat transfer would be difficult. By using Band-Models it is possible to replace these detailed calculations over frequency by an average over selected frequency intervals. A band model is used to relate the properties of a group of lines in the spectrum to the

properties of individual lines. The use of band models reduces considerably the computational time and complexity associated with estimating the physical properties of the turbulent exhaust gases.

In an early paper (H889/68), Huffaker described the main features of the band models for describing infra-red radiation from rocket exhausts. Band models may be said to originate by Elsasser in 1938. The mean emissivity of a band will depend on the particular shape for a single line, and the distribution of line intensities assumed in the model. Originally, Elsasser assumed an infinite space of equally intense lines. Another model by Mayer and Goody assumed that the lines in a band were completely random. This model is less dependant on the particular intensity distribution chosen. These models lead to the following mean emissivity functions:

a) For random model, if the lines are weak

$$\bar{\varepsilon} = 1 - \exp\left(-\frac{SU}{d}\right)$$

b) For random model, for strong lines

$$\bar{\varepsilon} = 1 - \exp\left[-2\frac{(S\gamma^0)^{\frac{1}{2}}}{d}(PU)^{\frac{1}{2}}\right]$$

where:
- $\bar{\varepsilon}$ = mean emissivity
- U = optical depth
- S = line intensity
- $P(S)$ = probability function
- $(\frac{1}{d})$ = line density
- γ = half-width

A band model, used because it is more realistic is the random model with exponential intensity distribution

$$\bar{\varepsilon} = 1 - \exp\left[-\frac{\frac{S_0}{d}U}{(1 + \frac{S_0 U}{\pi\gamma})^{\frac{1}{2}}}\right]$$

Huffaker used a modified Curtis-Godson approximation based on two special spectroscopic concepts, namely:

1) The molecular band model, and

2) Curtis-Godson approximation.

The band model yielded an explicit, closed formula for the molecular radiation within each selected spectral region of interest which used as input data the average line strength, the average line spacing, and the average line half width. The Curtis-Godson approximation was a method of combining the parameters that appear in the band model formulae in such a way that the parameters needed for an inhomogeneous gas calculation were obtained solely for homogeneous gas data. The modified Curtis-Godson approximation was used in the radiative heat transfer calculations which effectively averaged the band model parameters over the inhomogeneous path. This technique was shown to be accurate for strong gradients in temperature and concentration.

Reardon (R288/70) studied the application of band models to the prediction of radiant heat transfer (Liquid Propellants). The prediction method used absorption coefficients corresponding to weak line values with curves of growth developed using a random (or statistical) band model representation. The effective fine structure parameters used in the curves of growth to represent both Doppler and Collision broadening were evaluated for an inhomogeneous gas using a modified Curtis-Godson approximation. In this application the approximation was modified in the sense that it was applied to a spectral interval rather than a single spectral line.

Carbon particles in the rocket exhaust were treated as a gas since they were shown to be so small that scattering could be neglected, without appreciable error, for a total radiation calculation.

Band model parameters were obtained both experimentally and theoretically. Collision broadened line half widths were obtained from appropriate analytical expressions with coefficients based on experimental or theoretical data. Doppler broadened line half widths were obtained from a theoretical expression as a function of wavenumber, molecular weight and temperature.

$$b_{Di} = 5.94 \times 10^{-5} \frac{\omega}{m_i^{1/2}} (273/T)^{1/2}$$

where: m_i = Mol. wt. of i^{th} species

b_D = Doppler broadened line half-width

ω = wavenumber

The model here provided significant increases in operating capabilities and flexibility compared to previous models; however a problem existed in obtaining gas property data. Without realistic gas property data, the accuracy of radiation estimates remained uncertain.

Reardon later extended the above computer program to cover radiation from the following species; H_2O, CO_2, CO, HCl, HF, and carbon (R288/74). In addition an uncoupled two-phase program for radiation from Al_2O_3 was modified. The modified program was seen to have some shortcomings. Improvements recommended included,

i) a capability for using input data from a coupled solution for the gas-particle flow,

ii) a method for approximating a spectral distribution so total radiation could be predicted, and

iii) inclusion of some type of spatial integration.

A numerical infrared radiation bend model was developed by Harwell (H343/76,/77,/78) to predict the infrared spectral and spacial radiation intensity distributions in exhaust plumes. The model extended previous models which were developed for CO_2 from aircraft plumes to include water vapour radiation and the capability of treating high temperatures.

The computation of radiance from the plume was accomplished by dividing the plume into sufficiently small incremental blocks so that average conditions could be assigned and the blocks treated as homogeneous.

The plume was subdivided into slabs parallel to the line of sight. Each slab was then cut into horizontal strips along the line of sight vector. The radiation from each of these strips was computed by integration using the modified Curtis-Godson approximation.

2.3 Scattering Models

The approach by Freeman, et. al. (F855/79) was to use a scattering model in conjunction with the band model approach. Analytical models were developed with coupled gas-particle radiative transfer. The approach incorporated the following capabilities:

- coupled emission, absorption and scattering treatment
- multiple scattering with cylindrical geometry
- three dimensional, non uniform, axisymmetric medium
- arbitrary particle mixtures and size distributions
- arbitrary angular scattering phase function
- line by line and band model treatments
- alternate levels of engineering approximation.

The results included calculating for planar and cylindrical media using 6-flux, finite difference and Monte Carlo solution techniques. The calculations included the full range of optical parameters: optical depth, scattering albedo, phase function, medium geometry; and observables (transmissivity, reflectivity, emissivity; radiance and station radiance versus position and aspect).

The results demonstrated the importance of three dimensional multiple-scattering effects and the relative ability of different physical models to provide an accurate simulation. It was found that additional work was required in the areas of model optimization and application.

A survey of available optical parameters was made for particles of interest. Complex index of refraction data were not available for the following species: ZrC, B_2O_3, BN, BeO, Be_2N_2.

2.4 Gas Dynamics Models

The mixed supersonic and subsonic flow regions present in exhaust plumes does not appear to be adequately modeled at present. The usual approach is to commence with the constituative equations for conservation of mass, momentum and energy written in terms of turbulent flow using the accepted Reynolds' approach of mean plus fluctuating component. An appropriate equation of state and turbulent shear stress model is incorporated into the equations and the whole solved usually using a finite difference numerical scheme. Refined models may incorporate a turbulent kinetic energy turbulence model (H343/78) and consideration of chemical reactions (J51/75). The difference between the analytical solution and the finite difference equations is influenced by the step size of the mesh. This may need to be small to be stable and convergent. One of the major advantages of the finite difference approach is that the problem is reduced to an initial value problem with well defined boundary conditions. The main disadvantages lie in the requirement for a small step size requiring large computation times and computer memory, and that the complete boundary must be defined as a function of time.

The appropriate equations of motion are:

continuity:

$$\frac{\partial \rho}{\partial t} + \nabla \cdot \rho \vec{V} = 0$$

momentum:

$$\rho \left[\frac{\partial \vec{V}}{\partial t} + (\vec{V} \cdot \nabla) \vec{V} \right] = -\nabla p + \nabla \cdot \underline{\underline{\tau}}$$

energy:

$$\rho \frac{DE}{Dt} = \rho \frac{D\left[e + \frac{\vec{V} \cdot \vec{V}}{2}\right]}{Dt}$$

$$= -\nabla \cdot (p\vec{V}) + \nabla \cdot \underline{\underline{\tau}} \cdot \vec{V} - \nabla \cdot \vec{q}$$

Equation of State:

$$e = e(T, p)$$

Reynolds' Method:

Instantaneous value, = mean + fluctuating components:

$$\rho = (\bar{\rho} + \rho')$$

Laminar shear stress:

$$\tau_{ij} = \lambda \nabla \cdot \vec{V} \delta_{ij} + 2\mu \left(\frac{\partial V_i}{\partial X_i} + \frac{\partial V_i}{\partial X_j}\right)$$

The turbulent shear stress used by Harwell (H343/78) was based on the eddy diffusivity model of Donaldson and Gray for compressible free mixing of a primary jet with quiescent air:

$$\tau_t = -\bar{\rho}\,\overline{u'v'} = K\,\bar{\rho}\,L\,U_s\,\frac{\partial \bar{u}}{\partial r}$$

K is the mixing rate factor, L is a typical local length scale, ρ is the local density and U_s a typical velocity difference.

For axisymmetric flow, the turbulent kinetic energy conservation equation is

$$\rho\bar{u}\,\frac{\partial \bar{k}}{\partial X} + \rho\bar{v}\,\frac{\partial \bar{k}}{\partial r} = \left[\frac{\rho}{Pr_k}\,\varepsilon_k\,\frac{\partial \bar{k}}{\partial r}\right]$$

$$+ \rho\varepsilon_t\left(\frac{\partial \bar{u}}{\partial r}\right)^2 - a_2\,\frac{(\bar{k})^{3/2}}{\ell_k}$$

where $\bar{k} = \tfrac{1}{2}[(u')^2 + (v')^2]$

$$\varepsilon_t = \tau_t / \rho\frac{\partial \bar{u}}{\partial r}$$

$$\tau_t = a_1\,\bar{\rho}\,\bar{k}$$

$$Pr_k = \bar{P}\,C_p\,\frac{\varepsilon_t}{k}$$

a_1, a_2 are Universal empirical constants and ℓ_k a length scale for the turbulent kinetic energy.

3.0 PREVIOUS EXPERIMENTAL WORK

3.1 Introduction

This review of existing experimental studies is limited to infra-red radiation from rocket plumes. Although principally concerned with solid-fueled motors, some results from liquid fueled motors, especially hydrocarbon fueled (RP-1) motors, have been included.

3.2 Species Involved, IR Emission and Reactions

Habicht (H116/67) reported that the fine resolution, commonly observed in the line emission spectra of excited molecules, became smoothed with considerable overlap of the spectral curves due to the relatively long optical paths encountered in exhaust plumes.

Watson (W339/77) identified the principle emitting gases in the products of combustion of a solid metalized based propellant as CO, CO_2, H_2O, (and HCl). These species were typical of most solid and liquid propellant systems studied.

Eisel (E36/72) outlined the spectral details of these combustion products. He found that the CO_2 band occurred at about 4.3 μm and 2.7 μm. These bands corresponded to the ν_3 parallel antisymmetric stretching mode and a comination of the ν_1 and ν_3 parallel antisymmetric stretching and first overtone of the parallel bending mode.

H_2O bands occurred at 3.2 μm, 2.7 μm, 2.5 μm, 1.9 μm and 1.7 μm. These corresponded to the $2\nu_2$ first harmonic of the parallel bending mode, the ν_1 symmetric stretching mode, ν_3 antisymmetric stretching, $\nu_2 + \nu_3$ combination of fundamental bending and antisymmetric stretching modes, and $2\nu_2 + \nu_3$ combination of first harmonic of the bending mode and antisymmetric stretching mode respectively.

He found that HCl appeared at about 3.5 μm which corresponded to the fundamental stretching band. Finally it was found that the fundamental and first harmonic CO bands occurred at 4.6 μm and 2.3 μm.

Pai Verneker (P142/79) studied the reaction of ammonium perchlorate (AP) aluminium mixtures.

The stoichiometric equation used was as follows:

$$2.0\ NH_4ClO_4 + 3\tfrac{1}{2}Al \rightarrow 2.0\ HCl + 3.0\ H_2O + N_2 + 1^{2/3}Al_2O_3$$

The measured heat of combustion for the above reaction was 2.39 kcal/g. The standard values of heats of formation of AP, $H_2O(\ell)$, HCl used were 69.30, 68.32 and 22.06 kcal/mole respectively. The heat of formation of Al_2O_3 adopted was 400 kcal/mole. From the preceeding values, ΔH values for combustion were calculated.

He found, as expected, that the heat of combustion was seen to increase as aluminium concentration increased to stoichiometric composition after which it decreased.

Pergament (P439/71) gave an extensive list of mechanisms for afterburning in solid propellant plumes with recommended forward rate coefficients.

As stated by McCaa (M121/68) when particles were present in the exhaust plume, e.g. aluminium in solid propellant rockets, continuum radiation occurs. He found that this radiation was a function of both the number concentration of solid particles present and their temperature.

3.3 Effect on Infrared Radiation of Aluminium Particles

It was reported by Zirkind (Z82/66) that the addition of aluminium in metallized-base propellants gave rise to continuum radiation from the aluminium oxide particles in the exhaust plume.

Along the same lines, Habicht (H116/67) stated that the radiation emitted from aluminium oxide, or from the oxides of other metals which may be present in a propellant, lay in the "atmospheric window" region of the spectrum (7-15 microns) where little absorption took place. In this region it was also found that scattering decreased because the wavelength of the radiation was greater than the mean diameter of particulate matter in the atmosphere.

Habicht also noted that if a propellant contained aluminium, with a high oxygen affinity, then the oxygen available for formation of H_2O and CO_2 was reduced relative to a non-metalized propellant. A decrease in the amount of H_2O and CO_2 formed should then be observable as a decrease in the energy radiated in the H_2O and CO_2 bands of the infrared combustion emission spectrum. To our knowledge this inference requires experimental confirmation.

Reiger (R554/79) reported measurements on the IR emission intensity of alumina particles in rocket exhaust gases. He observed large discrepancies between the emissivity of pure macroscopic samples of alumina and corresponding particles in the exhaust gases. He attributed this difference to incomplete oxidation of the aluminium in the oxygen defficient combustion.

He found that earlier plume radiation models used phenomenologically determined and relatively large values of particulate emissivity in order to bring predictions into agreement with data. Despite discussion of the physical mechanisms responsible for producing these relatively large values there is no consensus as to the dominant mechanism.

Reiger observed that much of the aluminium combustion took place in large droplets (40-800 μm) of aluminium/alumina migrating around on the propellant surface. This would result in droplets of unburnt aluminium, some encapsulated, being injected from the chamber.

It was found that small amounts of aluminium (a few % by volume) lead to relatively large values for composite emissivities. He concluded that small amounts of unburnt aluminium contained in or on rocket exhaust alumina would go a long way to explaining the discrepancies between measured pure alumina emissivity and the large amount of infrared particulate emission typically seen from aluminized solid propellant rocket plumes.

Similar observations by Worster (W931/75) were attributed to changes in crystal structure and impurities in the aluminium.

3.4 Other Particles

Cohen (C678/71) confirmed that the addition of 2% copperoxide (I) to an aluminized solid propellant was very effective, since it improved the ignition and combustion of the aluminium.

He discovered that the addition of the copper oxide

1) produced a higher regression rate of the burning face than recorded without the catalyst,

2) produced a faster ignition of the aluminium, and

3) created a marked lowering of the limiting combustion pressure.

Cohen stated that the oxidation of Cu_2O yielded a considerable amount of energy:

$$Cu_2O + \tfrac{1}{2}O_2 \rightarrow 2CuO + 29.9 \text{ kcal/mole}$$

He found that this energy fed back to the surface by conduction increasing the surface temperature and, consequently, the burning rate.

Examination after combustion showed that more significant amounts of hydrogen chloride and chlorine were formed. These two gases promoted the ignition of aluminium. By breaking down the thin oxide coating on the aluminium particles.

Cohen also studied the combustion of ammonium perchlorate/magnesium mixtures. He stated that magnesium, in contrast to aluminium, was a volatile metal. He found that smooth combustion occurred under less limiting conditions than that of AP/Al. For instance these mixtures were infact found to burn smoothly at sub atmospheric pressures as well as higher pressures.

Llinas (791/69) observed that in liquid hydrocarbon fuels carbon particles produced a continuum emission.

He found that measurement of the carbon particle sizes in both full-scale and model engine exhaust plumes indicated that the mean carbon particle radius was ≈20 mm and a carbon particle mass fraction of 0.02 could be reasonably assumed.

3.5 Size Distribution of Al_2O_3

Particle size and distribution are important in determining exhaust emission levels.

Freeman (F855/79) noted that rocket exhaust plumes did not, in general, consist of particles with only one fixed size. He therefore stated that it was necessary to investigate the characteristics of size distributions.

Gany (G195/79) studied the combustion and agglomeration process of aluminium particles emitted from the surface on an aluminized double base propellant. He found that the mechanism of Al/Al_2O_3 burning consisted of the particles forming on the surface of the propellant, moving along the surface and entering the flow field.

It was found that burning agglomerates and particles formed two identifiable particle distributions. The larger particles being mostly in the 40-800 μm size range and the very small particles generally smaller than 10 μm. He found that the distribution of smaller particles, which included the Al_2O_3 smoke, tended to follow the gas velocity without lag. However, it was found that their diameter in the flame could not be determined with certainty due to the turbulence intensity of the flame. Particle size was determined by trapping and measuring the particles in the cooled exhaust.

Gany found that the following parameters decreased with increasing chamber pressure: collision frequency on the surface, the agglomerate residence time on the surface, and mean agglomerate size. It was also discovered that increasing the cross flow velocity also caused a decrease in the mean agglomerate size.

The size of aluminium particles used in the solid propellant was found to affect burning characteristics. The large aluminium particles burned without the aluminium igniting or agglomerating on the surface.

Worster (W931/75) reported that for rockets with throat diameters above 5 inches the mean-mass particle radius lay in the range 4-8 μm. It was found therefore that particle radius, r, was of importance because, as predicted by the well-established MIE theory, emission at a given wavelength, λ was inhibited by geometric consideration when $2\pi r/\lambda > 1$. This was not the case for the wavelengths of interest and the particle distribution encountered.

Vanderbilt (V288/76) stated that the scattering effects of particles became important when the particle diameters were equal to or greater than the wavelength of interest. This was the case for metalic oxides such as Al_2O_3 in solid propellant combustion.

MIE parameter, $\alpha = 2\pi r/\lambda$

λ = wavelength of radiation

r = radius of particles

Particles for which $\alpha \ll 1$ did not scatter appreciably and adsorption (and emission) in this region was adequately described by the Rayleigh theory where particles are treated as a pseudo-gas.

When α was equal to (or moderately greater than) units, scattering became important.

For solid propellant exhaust species r was typically in the range 0.5 → 5.0 μm.

When $\alpha \ll 1$ irregularities in particle shape became comparable to the wavelength of radiation, and the MIE theory broke down.

3.6 O/F Ratio and Choked Flow

Roux (R554/78) measured radiant intensity for a variety of test cell and nozzle afterbody conditions including tunnel Mach number (M), combustor nozzle exit exhaust gas temperature (TG), Fuel to air Ratio, and nozzle pressure ratio (NPR) which is the ratio of combustion chamber pressure to free stream static pressure.

He found that the variation of nozzle pressure ratio and nozzle exit exhaust gas temperature produced a strong variation in the radiance level and radiance distribution in the exhaust plume. An increase in TG from about 1500°F to 1800°F resulted in a six fold increase in radiance level. An increase in NPR caused a strong influence on the flow field Mach disc structure; this resulted in a widely varying radiance distribution and intensity level.

Roux found that opposed to the strong influence of nozzle pressure ratio and nozzle exit exhaust temperature on the radiation field, the free stream Mach number change showed only a weak influence on the radiation field. He found that there was only a slight increase in the radiance level at the first Mach disc as the free stream Mach number was increased.

Rothschild (R847) studied the IR emission from hydrocarbon exhausts. Fuels used were RP-1, C_2H_4, CH_4 and C_6H_6 (commercial grade or better). These were burnt in a AFATL Rocket with gaseous oxygen (commercial grade).

He discovered that the peak specific radiant intensity in the 4.1 to 5.1 micrometer band increased as the fuel C/H ratio increased and as the fuel's combustion efficiency decreased. It was found that regardless of fuel type, the most dramatic effect on specific radiant intensity was O/F ratio. The peak specific radiant intensity was found to occur at or near one-half the stoichiometric O/F. The specific radiant intensity decreased exponentially with increasing O/F and dramatically with decreasing O/F relative to the peak O/F value.

He found that the spacial distribution of plume radiation in the 4.1 to 5.1 micrometer band was also dramatically influenced by mixture ratio. Fuel-rich mixture rations resulted in peak radiation intensities up to 60 cm downstream from the nozzle exit. Oxidizer-rich mixture ratios had peak radiant intensities at or near the nozzle exit.

Rothschild found that plume spectral distributions at oxidizer-rich mixture ratios showed characteristic vibrational-rotational bands for H_2O and CO_2 as expected in hydrocarbon flames. At fuel rich mixture ratios, the infrared spectra indicated products of incomplete hydrocarbon combustion. For CH_4 the fuel-rich spectra showed emissions at 3.3 to 3.4 micrometers from unburnt CH_4. For C_6H_6 the fuel rich spectra showed continuum emissions from soot. It was found that at O/F ratio of 2.0 the continuum portion of the C_6H_6 became important. At very fuel rich conditions (O/F = 1.5) the C_6H_6 spectrum was dominated by continuum radiation. The IR spectra of RP-1 and C_2H_4 did not yield clues to incomplete combustion products. However, visual observation did show incandescent soot in the plumes of all four fuels at low O/F.

Rothschild stated that the above results could be interpreted in terms of various effects on plume afterburning. He found that the amount of combustible species for plume afterburning increased as O/F and C efficiency decreased. However, there was a point at which further reduction in O/F ratio, while adding more combustible species, brought the plume flame temperature below the flammability limits, which resulted in drastic decrease in afterburning. The variation in specific radiant intensity with fuel C/H ratio could be explained in terms of the CO_2 which dominated the radiation in the spectral band of interest. Higher fuel C/H ratios yielded more CO_2 which resulted in more radiation.

Rothschild stated that questions still remained unanswered about the IR processes of hydrocarbon plumes.

These included

- What were the products of incomplete combustion and how might they be varied.
- What role did soot play in the radiant transport processes in the 4-5 μm range.
- What were the mechanisms for soot production and oxidation.
- What were the speci, temperature, and velocity distributions.

He concluded by saying that further experimentation was necessary to clarify these questions.

Harwell (343/76) studied the infrared radiation characteristics of a hot gas generator: using a small kerosene/O_2 rocket. He found that the character of the axial distribution of radiation significantly changed when the O/F ratio was varied from 2.0 → 3.0. At lower O/F values the peak radiation occurred 7.0 to 12.5 nozzle radii downstream from the nozzle exit.

Within the plume it was discovered that although hot spots existed, most of the radiation was found to occur in the afterburning and/or mixing layer portion of the plume. He found that at values of O/F ratio greater than 3, the peak value of the radiation intensity was located immediately downstream of the first shock, usually within 5 mm of the nozzle exit, however the majority of the total radiation was still from the after-burning plume.

He determined that the total radiation from the whole exhaust plume was quite sensitive to the engine O/F value. It was observed that the radiant intensity had a pronounced maximum at an engine O/F value of 2.0 (the real value may have been slightly higher because of entrained external oxygen.

Ebeoglu (E16/74) stated that the major parameter which controlled the infrared radiation from a plume was the O/F ratio. The radiant energy ($\overline{J}$) was expressed in normalized units (watts/steradian/gram/second) and was used to relate radiant intensity (watts/steradian) to the combined mass flow of the oxidiser and fuel into the engine (g/sec). It was found that maximum energy ($\overline{J}$) was produced at an O/F ratio well below the stoichiometric ratio of 3.4 for the kerosene/oxygen mixture. The value of O/F ratio at which maximum $\overline{J}$ occurred increased with altitude.

He concluded that afterburning was a major mechanism in the creation of radiant energy. The combustion process in the engine was found to provide only part of the oxidation required. Maximum radiation was not produced when the engine was operating with a stoichiometric mixture.

Maximum radiant energy was found to be produced when a fuel rich mixture existing from the engine nozzle, reacted with the oxygen in the air. This was in agreement with Harwell (H343/76).

Ebeoglu (E16/74) also studied the effect of choked flow on radiant intensity. He found that the infrared intensity of an exhaust plume changed drastically depending whether or not choked flow existed.

Choked flow existed for supersonic flow (M>1) and the flow was unchoked when subsonic.

The throat pressure drop for choked flow was given by the standard equation:

$$Pc/Pe = \left[1 + \frac{V-1}{2} M^2\right]^{V/(V-1)}$$

Pc = chamber pressure V = specific heat ratio

Pe = ambient exit pressure M = Mach number

He found that even though V varied with temperature and pressure, an average value of 1.26 could be used without significant error. Thus when M = 1 the equation above reduced to Pc = 1.808 Pe.

It was found that when the engine chamber pressure fell below this critical value the exhaust character and radiant intensity of the plume changed quite drastically.

Ebeoglu concluded that order of magnitude variations in plume IR intensity were caused by two major parameters - oxygen to fuel mixture ratio and the existance of choked flow.

3.7 Other Parameters Effecting IR Radiation

From results obtained from a small kerosene/oxygen rocket Harwell (343/76) found that the magnitude of the infrared radiation varied in both axial and radial directions in the exhaust plume. The maximum value of the radiation, at a fixed axial position in the radial direction, was found to be at the jet centreline. He found that the radiation varied in the axial direction and the existance of radiating zones ("hot spots") behind the shock waves was confirmed experimentally.

It was discovered that experimental measurements at higher chamber pressures would be needed to ensure that the nozzle was completely filled. The spectral distribution of the radiation indicated that the principle radiation was in the 4-5 μ band from the hot carbon dioxide and water vapor.

Ebeoglu (E16/74) experimentally showed that radiant intensity was directly proportional to total mass flow rate.

It was shown that chamber pressure was related to mass flow rate as follows:

$$v = \frac{PcA}{\dot{M}}$$

v = characteristic velocity
Pc = chamber pressure
A = throat area
$\dot{M}$ = mass flow rate

From the equation it could be seen that Pc was directly proportional to $\dot{M}$.

These two parameters, of chamber pressure and the total mass flow rate, would therefore cause linear variations in radiant intensity.

Ebeoglu also carried out experiments concerning exit gas velocity and thrust and their effect on IR radiant intensity. It was found that little variation in radiant intensity occurred with variations in exit gas velocity or thrust.

4.0 PREVIOUS EXPERIMENTAL APPARATUS

4.1 Instrumentation

Eisel (E36/72) used a rapid scanning spectrometer to follow concentrations and temperature of combustion products of ammonium perchlorate (NH_4ClO_4) - Polyurethane propellants. The instrument was capable of scanning rates from 8 scan/second. During the study it was operated in the 1.7 μm to 4.8 μm wavelength range and at 1.0 millisecond per scan. Entrance and exit slits were set at 0.5 mm.

In addition to the spectrometer, a radiation source unit in which a silicon carbide globar was located, was used. It could be controlled to within 4°C at temperatures from 1000°C to 1225°C. This provided a means of doing absorption spectroscopy. The external radiation beam was interupted periodically in synchronization with the scanning of the receiver to provide alternate emission and emission-absorption information. The detectors used were solid state InAs and InSb.

Harwell (343/76) in his study of the exhaust plume of a small kerosene/oxygen rocket made use of several instruments in detecting radiant energy.

The primary instrument used to obtain total radiation intensity measurements was a radiometer. The spectral range was 2.5 to 5.1 μm and the detector used was liquid nitrogen cooled InSb.

Spectral data in the 2.6 to 5.4 μm range were obtained using an interferometer spectrometer. This instrument had a 4 inch cassegrain optical system, step variable field of view and resolution settings and a cooled InSb detector.

The instrument was placed 42 feet from the engine plume and boresighted to a 2X rifle scope which was used for alignment.

The interferometer was calibrated using a 600°C collimated laboratory blackbody. A 16 mm recording camera system was used to photograph the visible plume structure.

Klein (K64/67) used a rapid scanning spectrometer to study emissions from rocket exhaust plumes. It operated in selected spectral regions from ultraviolet at 2500 Å to infrared at 15 μm. The spectrometer viewed the plume through a sapphire window located in a vacuum tank wall. The optical path was flushed with dry nitrogen to eliminate interference from atmospheric CO_2 and H_2O.

In the rapid scanning spectrometer the wavelength scan was accomplished by sweeping corner mirrors through a focal plane. This design inherently provided for simultaneously scanning two contiguous wavelength intervals. Two exit slits and two detector systems were used.

The short wavelength region covered was 1.6 to 3.2 μm using an Indium Arsenide Detector cooled with dry ice. The long wavelength region 3.0 to 5.0 μm was covered with a liquid

nitrogen cooled InSb detector. Scan times varied from 100 to 1 msec. per scan.

Martin (M379/74) used an infrared imaging camera to obtain measurements from exhaust plumes. The imaging and data aquisition system consisted of an infrared camera interfaced to a nine track digital tape recorder.

The system incorporated three subsystems:

1) infrared camera,

2) camera control monitor, and

3) digital data aquisition.

The camera optical system utilized two moving flat mirrors. A rotating drum mirror scanned the horizontal field of view and a tilting mirror swept vertically. The sweep rates of the two mirrors differed by a factor of 94. Thus for each vertical sweep of the tilting mirror, there were 94 full horizontal sweeps by the rotating mirror.

The radiation to be measured was reflected by the scanning mirrors into a concave mirror which focussed the source radiation onto a photovoltaic detector. This detector translated incident ratiant energy to an electric video signal that was representative of the source radiation.

Roux (R554/78) used an IR scanning camera to measure radiance from a rocket plume. The instrumentation consisted of a scanning infrared imaging camera, calibration black body, and CO_2 spectral filter (4.21 - 4.41 μm). The IR camera system was equipped with an InSb detector (sensitive in the 2-5.5 μm region). Scanning was achieved by two rotating prisms. The vertical prism rotated at a rate of 2 hertz while the horizontal scanning prism rotated at 200 hertz. Each vertical scan therefore included 100 horizontal scans and constituted one complete frame of data.

Rothschild (847/76) used an infrared scanner system to measure the infrared plume spacial distributions and integral plume apparent radiant intensities of a small rocket exhaust plume. The infrared scanner system consisted of an infrared camera and camera control monitor with a digital data aquisition system interfaced to a 9-track digital tape recorder as used by Martin.

A photovoltaic Liquid N_2 cooled InSb detector was used. The plume was viewed through a sapphire window located in the vacuum chamber.

The infrared plume spectral distributions were measured with an Interferometer Spectrometer capable of two wavenumber resolution. The instrument used a mini computer for real time data acquisition and fast fourier transform data reduction. Both an uncooled PbSe detector and a cooled (77°K) InSb detector were used for the spectral range of 2-5 micrometers.

4.2 Burner Design

Eisel (E36/72) used a modified Burner. Instead of using fixed length interchangeable burner bodies the burner was provided with an infinitely variable threaded section which was calibrated and provided continuous variation of free volume.

Windows were installed on opposite sides of the burner to allow both viewing of emitted radiation and viewing of radiation from the source unit from the opposite side of the burner. The window material used was exclusively 3.17 mm thick sapphire. The transmissivity of the sapphire over the wavelengths of interest (1.7 - 3.5 μm) was determined experimentally.

Eisel found that it was necessary to provide a means of keeping the products of combustion from condensing on the window surface. A gas flushing system was used whereby gas at relatively high pressure was introduced into a manifold within the burner from which it flowed from an orifice on the upstream side of each window and out into the combustion chamber. Air with CO_2 and H_2O removed was used.

Harwell (H343/76) used a kerosene/gaseous oxygen rocket engine in his experimentation. The rocket engine consisted of a water cooled stainless-steel cylindrical chamber (0.78 inches diam. x 1.620 inches long) with interchangeable nozzles. Mixing and atomization of the fuel were accomplished using a premix injector. Gaseous oxygen was introduced into the injector behind the kerosene and was used to drive the kerosene/gaseous mixture through a 0.055 inch diam. orifice to aid in mixing and atomization. Tungsten was used for the injector tip. Ignition was carried out by a spark plug ignition system.

The small rocket was capable of operating at chamber pressures up to 200 psi and at oxygen mass flow rates in the 2 to 10 gm/sec. range and kerosene mass flow rates of 0.2 to 4 gm/sec.

Klein (K64/67) used a short duration test facility. These were based on shock-tube techniques. Model rocket engines were fired in an evacuated chamber which simulated high altitudes, and provided hot steady flow for approximately 5 msec. He used two types of nozzles. A $\frac{1}{25}$ scale J-2 nozzle burning H_2/O_2 at an O/F ratio of 5.5 and a $\frac{1}{45}$ scale F-1 nozzle burning ethylene/O_2 at an O/F ratio of 2.25.

4.3 Ancillaries

To obtain the spacial distribution of radiant intensity in the exhaust plume, Harwell used a moveable shield and moveable engine support. The moveable shield assembly, which consisted of a plate with a small diameter hole, was moved in the vertical direction by a reversible drill motor. This arrangement permitted the small aperture to move in a vertical direction across the plume at a fixed horizontal position downstream of the nozzle.

Horizontal displacement of the engine relative to the aperture was accomplished by mounting the engine on a beam that could be translated using a reversible drill motor.

5.0 AREAS WHERE FURTHER RESEARCH WORK IS NEEDED

5.1 Particle Size

Difficulties and inconsistencies are apparent in determining Al_2O_3 particle size distribution in plumes from metallized solid-fuel propellants. The size distributions reported seem to be determined more by the method of particle collection and size analysis than by the size of the Al fragments in the solid fuel. Observed particle sizes occur in the range 0.1 to 100 μm, with the greatest population in the decade 2 to 20 μm. This corresponds with the IR wavelengths of interest (namely 3-14 μm) thus, according to the Mie theory, there is maximum interaction between the electromagnetic radiation and particle clouds when particle size approachs the wavelength of the radiation. Both attenuated and enhanced emission have been observed under these conditions. (D747/77)

It is thus important to investigate and quantify the effect of particle size on radiant emission. To this end a method needs to be developed for sampling and measuring particle size distribution in the exhaust plume.

Other aspects of this work which merit attention are

(i) the mode of combustion of the aluminium flakes in the fuel, both in the motor and possibly in plume.

(ii) the factors determining alumina (Al_2O_3) size and distribution in the plume and any variation with position.

(iii) possible sintering, agglomeration, and fragmentation effects within the motor and plume.

(iv) data on the optical properties of some particulates encountered in plumes are incomplete - such as complex refractive index for ZrC, B_2O_3, BeO, BN and others.

5.2 Plume Composition

The band models appear to be moderately successful in describing radiant emission in the absence of particles. This accuracy being limited either by the band width chosen - as dictated by the computing power available - or by the lack of knowledge of the concentration distribution of radiating and absorbing species and their temperature. More serious discrepancies arise when particles are present in the plume with both under - and over - prediction of intensities, (particularly in 4-5 mm range) occuring. The work by Jensen and Wilson (J51/75) is particularly encouraging - but their model did not include the effects of shock waves or condensed species. There was room for improvement in kinetic data, particularly in some of the initiation and recombination reactions as well as in turbulence mixing parameters. More accurate information on the dissipation term in the turbulent

kinetic energy (TKE) transport equation is needed for more accurate predictions. A substantial change in nozzle exit temperatures is predicted with certain metal-containing additives (e.g. Sn, K).

5.3 Flow Structure of Plume

Current plume models incorporate a treatment of shock waves and are considered reliable in the absence of significant particle loading. Additional information is needed on turbulent diffusivities and the coupling between gaseous and condensed phases.

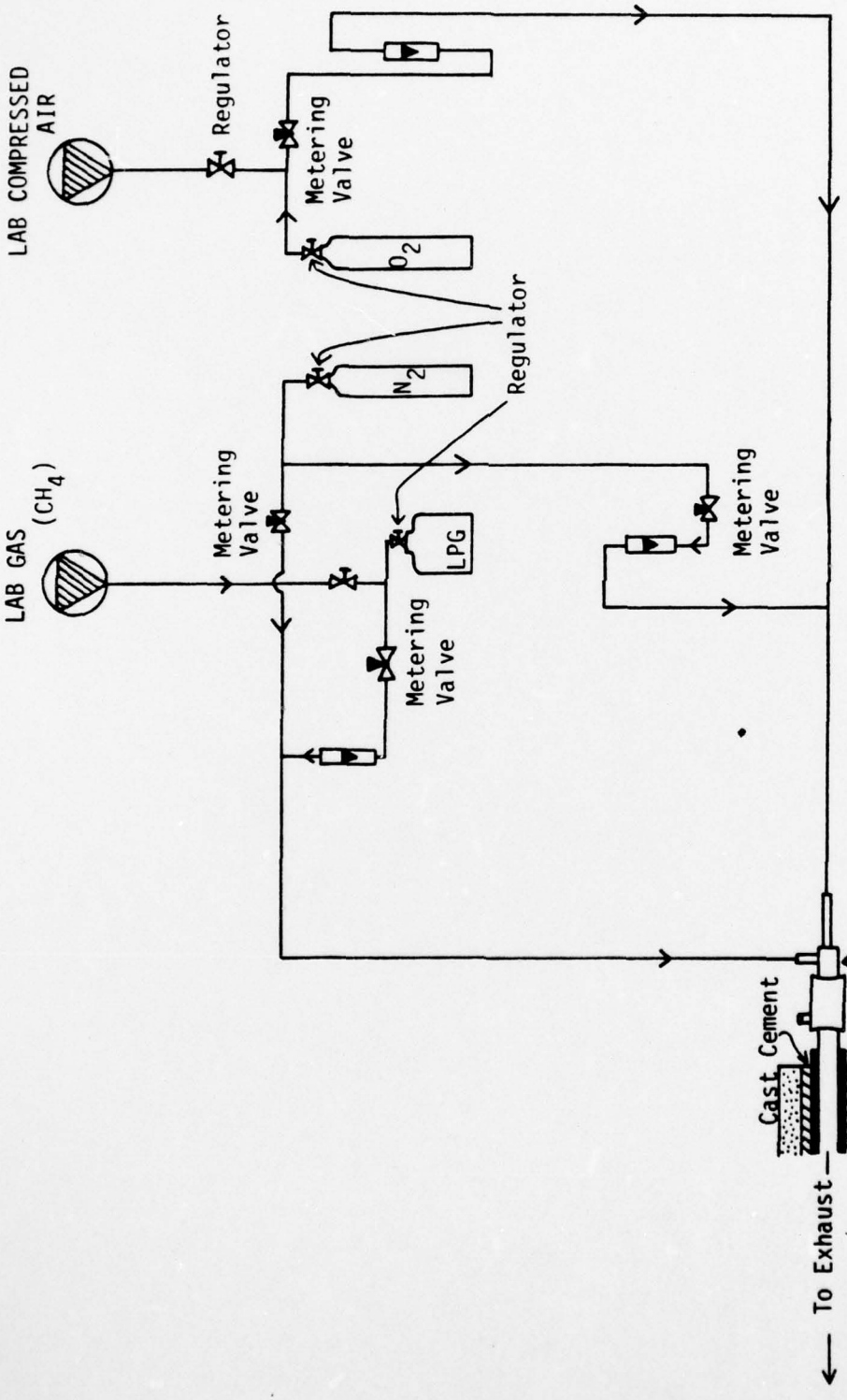

Figure 1: General Arrangement of Hot Flame Experimental Rig Showing Gas Flow Circuits.

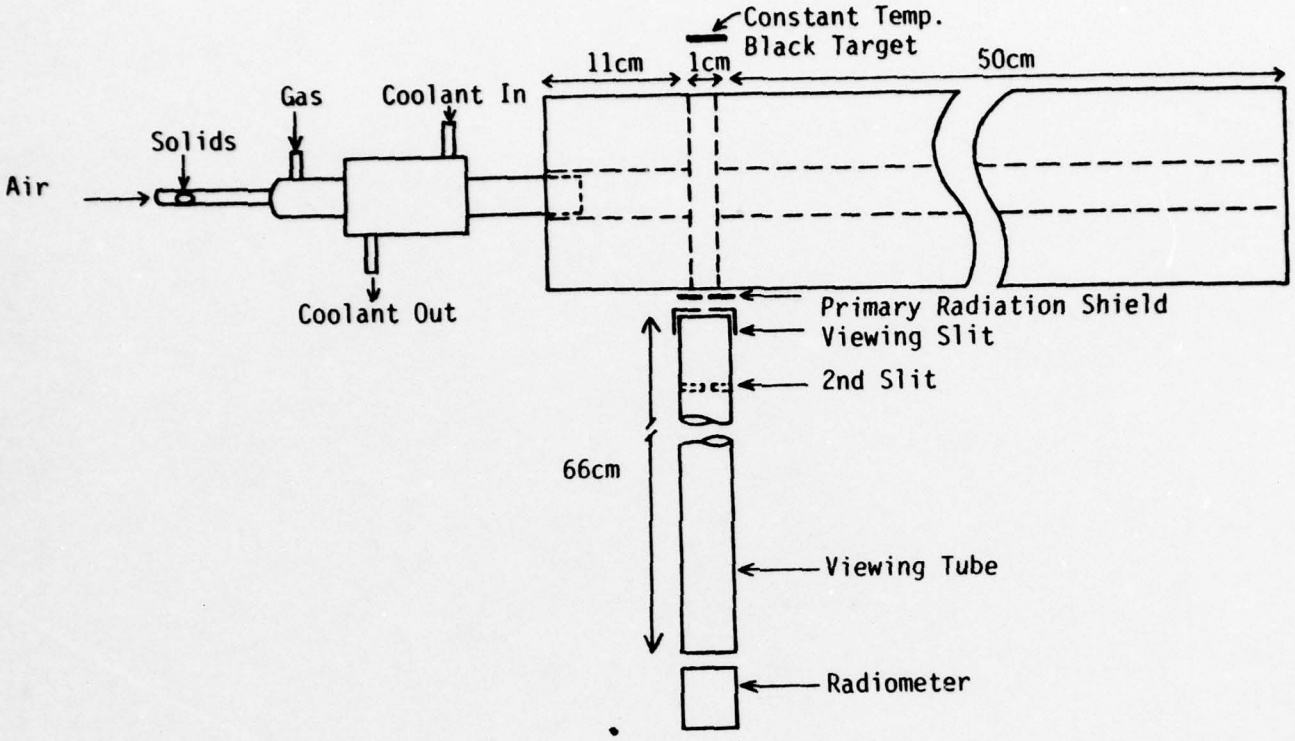

Figure 2: General Arrangement of Burner, Combustion Tube and Radiometer.

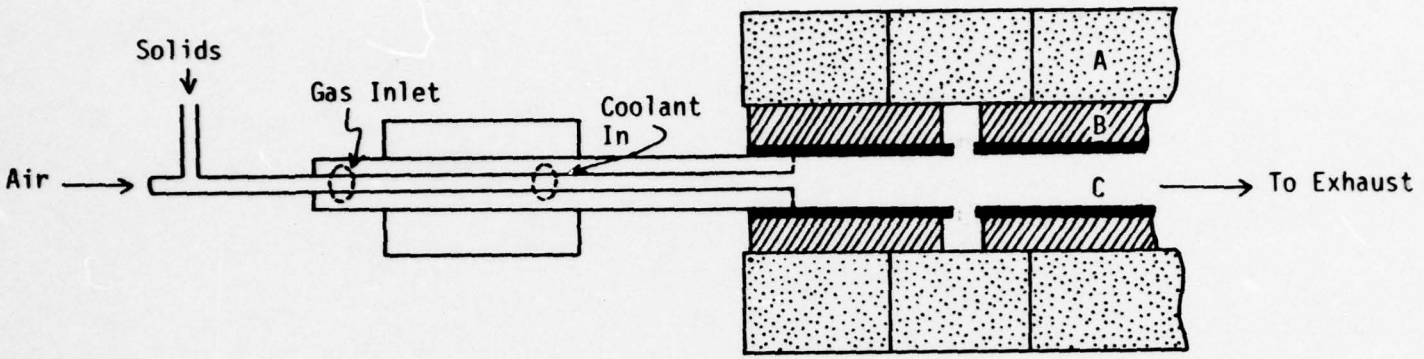

A: Fire Bricks

B: Cast High Temperature Cement as support for Alumina Tubing

C: Recrystallized Alumina Tubing

Figure 3: Section through Burner and Combustion Tube showing solids/fuel/air flows in burner and method of supporting Combustion tube. For axial emission profiles, the burner was moved inside the combustion tube. The gap can be seen in the combustion tube for radiometer viewing.

6.0 EXPERIMENTAL PROGRAM

In the light of the literature review, it was decided to concentrate the experimental program on measuring the effect of alumina particle addition to a plume. The wavelength ranges of interest correspond to high CO, CO_2 emission coupled with low H_2O absorption viz. 3-5 μm and 8-14 μm. Particle in plumes are in the Mie size range and can have optical properties quite different from the usual black - or gray - body behaviour of larger particles. (D747/77) Modification of the IR signiture by appropriate modification of the propellant to produce condensed species is a possibility. In any case good data are required to check existing plume models.

In view of the reported inconsistencies in measurement of particle size distributions, it was thought advantageous to incorporate provision for particle sampling for subsequent size analysis - with a view to developing a reliable procedure for hot particle sampling.

6.1 Gas Flame Burner

The rig was designed to burn a hydrocarbon gas (either LPG or N.G.) in air with provision for oxygen enrichment to boost flame temperature as required. The burner design required some development. It was important to produce a turbulent combustion flame to better simulate conditions in an actual exhaust plume, this required premixing of fuel and oxidant before ignition. In addition, Al_2O_3 particles had to be added to the unburnt gas stream in a uniform and controlled manner (i.e. the system had to be "stiff" and free from low frequency pulsations due to the solids addition). Further, the uniform distribution of the solids in the mixed gas had to be preserved on ignition. This latter requirement has only been partially met in the latest burner design. The problem arises when the sudden expansion of the mixed gases at the burner mouth, which is needed to reduce the gas velocity to below the flame velocity for stable combustion, results in the particles preferentially staying in the core region of the flame since their inertia causes them to lag behind the gas expansion. This fault is not considered a serious draw-back since it produces a two-phase flow not unlike that in the divergent section of a rocket exit nozzle.

The burner shown in figure 1 is not the latest design. It was used for the early preliminary work. All work to date has been obtained with this burner. It incorporated a central air line with a venture 'T' section for solids addition. Fuel gas was not premixed with air prior to combustion but rather exited from six holes in the face of the burner. Mixing of the two gas streams occurred in the annular combustion zone. This thus gave rise to diffusion flames originating at each of the six fuel ports, and a cold central core which also contained the bulk of the added particles. A modified dump combuster (C552/80) is currently being fabricated which is expected to overcome the shortcomings of the earlier burner. The new burner incorporates an auger solids feeder and premixing of solids, fuel, and air/oxygen streams prior to combustion.

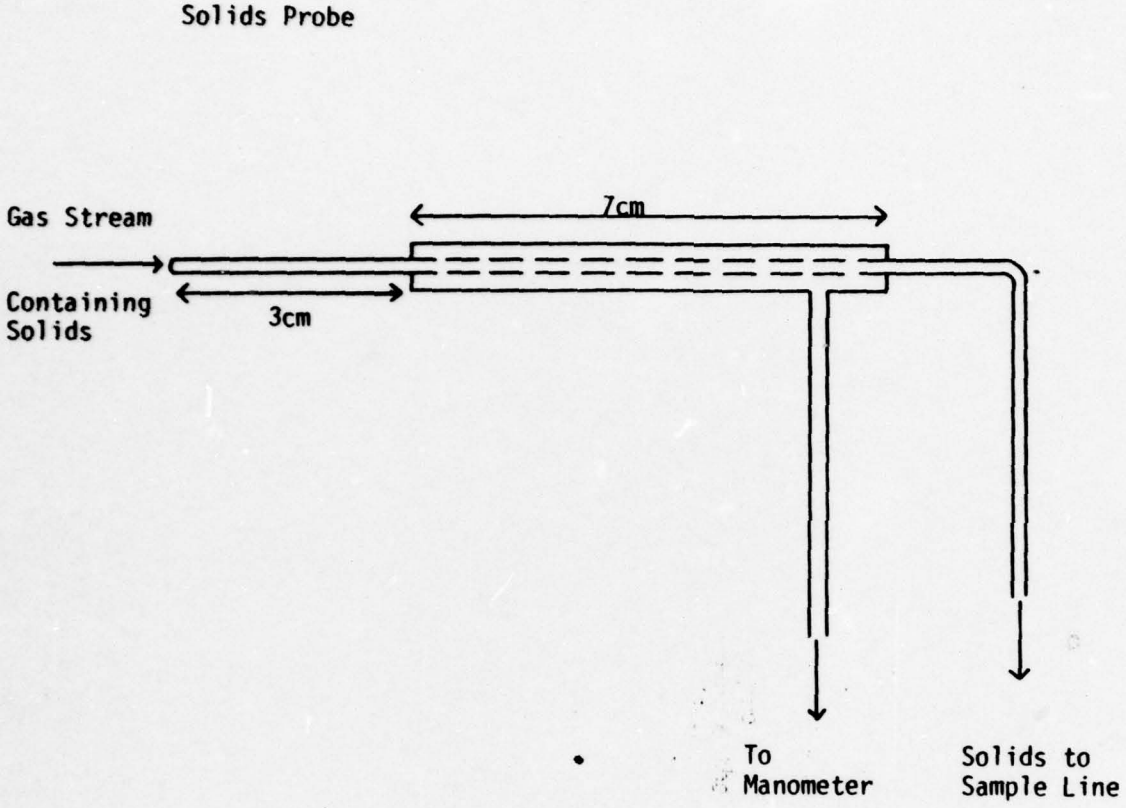

Figure 4: Isokinetic Sampling Probe for Solids Collection.

Detail of Sampling Line

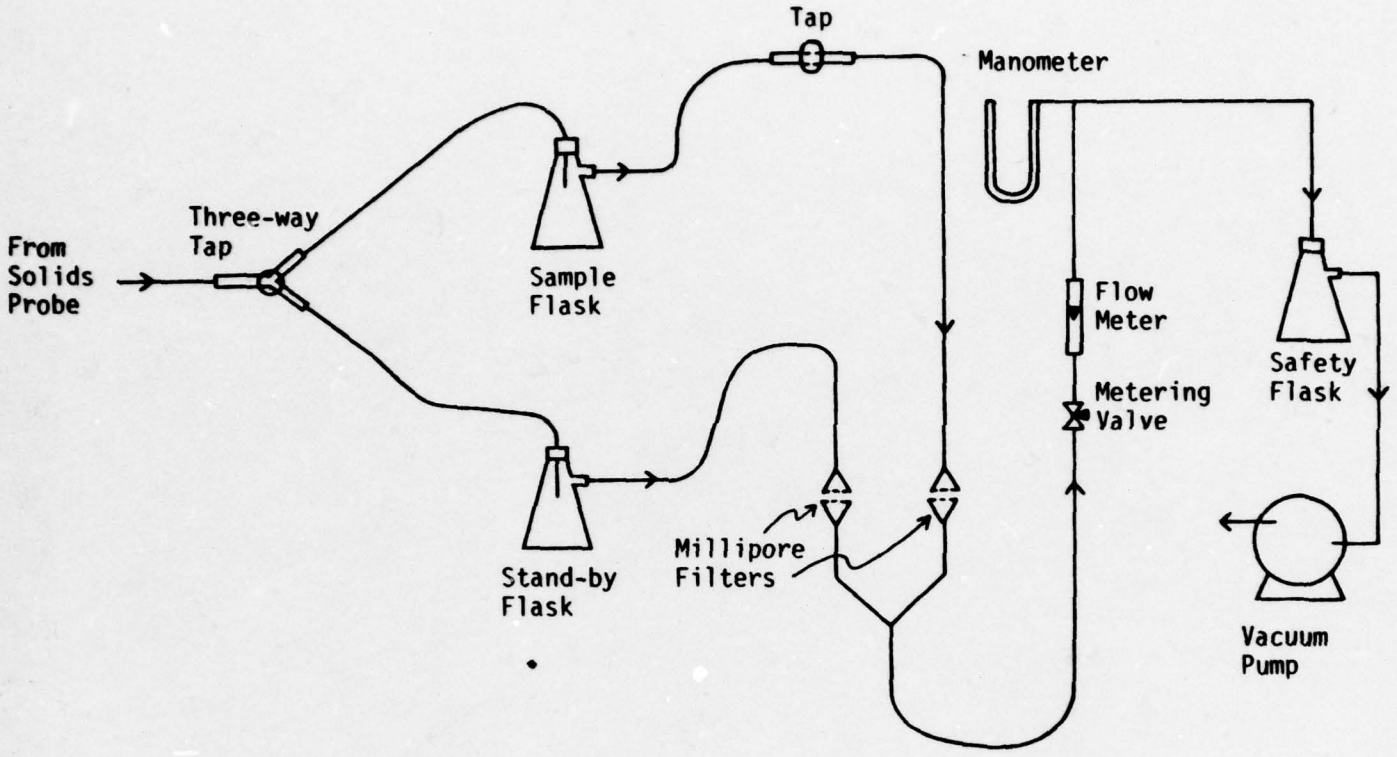

Figure 5: Solids Sampling System for Particle Collection.

6.2 Combustion Tube

Emissive intensity is temperature dependant. Hence heat loses from the flame and particles must be minimised so that the planned axial radiation intensity profiles measured the extent of the combustion reactions and interphase energy coupling and not just radiant energy loss from the flame. A ceramic tube of recrystallized alumina was chosen to contain the flame, having good high temperature stability. The tube was supported in moulded cast ceramic saddles and the whole enclosed in fire-brick. Warm-up time was of the order of 90 min. Once the tube temperature exceeded the gas ignition temperature, stable combustion resulted.

A viewing window was provided in the tube by cutting off a short length and separating the break by about 5 mm. To ensure that no flame or combustion gases escaped from this gap, (due to the back-pressure of the remainder of the tube) an exhaust extractor fan was used. The draw by the fan was adjusted to ensure that flame had a constant diameter across the gap and neither lost gases to the atmosphere nor entrained ambient air. Profiles were obtained by moving the burner inside the combustion tube and keeping the radiometer fixed. For temperature profiles, the thermocouple was traversed.

6.3 Radiometer

A radiometer was chosen to measure infrared radiant intensity using filters to isolate the bands of interest. Due to delays in delivery of the instrument (5 mo.) a similar but superceeded model was obtained on loan and used for the early work. The borrowed instrument was uncalibrated and lacked suitable filters.

The instrument now available is a Molectron PR200 radiometer with lithium tantalate pyroelectric detector. Instrument sensitivity ranges from 2.0 μW to 200 mW f.s.d. Spectral range of the detector is 0.2 to 20 μm (±3%) with an upper limit of 400 nm. Filters available are quartz, (.23-3.5 μm), sapphire (0.3-5 μm), and germanium (8-14 μm). The absorption spectra of these filters measured in our laboratory are given in figure 6, 7, 8.

The detector has a nominal field of view of 0.1 steradian which is wider than that required. To eliminate pick-up of unwanted radiation, a blackened viewing tube with collimating slits was used. Slit width was 2 mm. The tube was purged with air to control temperature build-up. Behind the flame was a black-body viewing target, air cooled as for the viewing tube. Before flame ignition, the radiometer was zeroed on this target. Tube alignment was by line of sight thro the viewing slits with the radiometer temporarily removed. When in place, an insulated enclosure surrounded the detector and chopper.

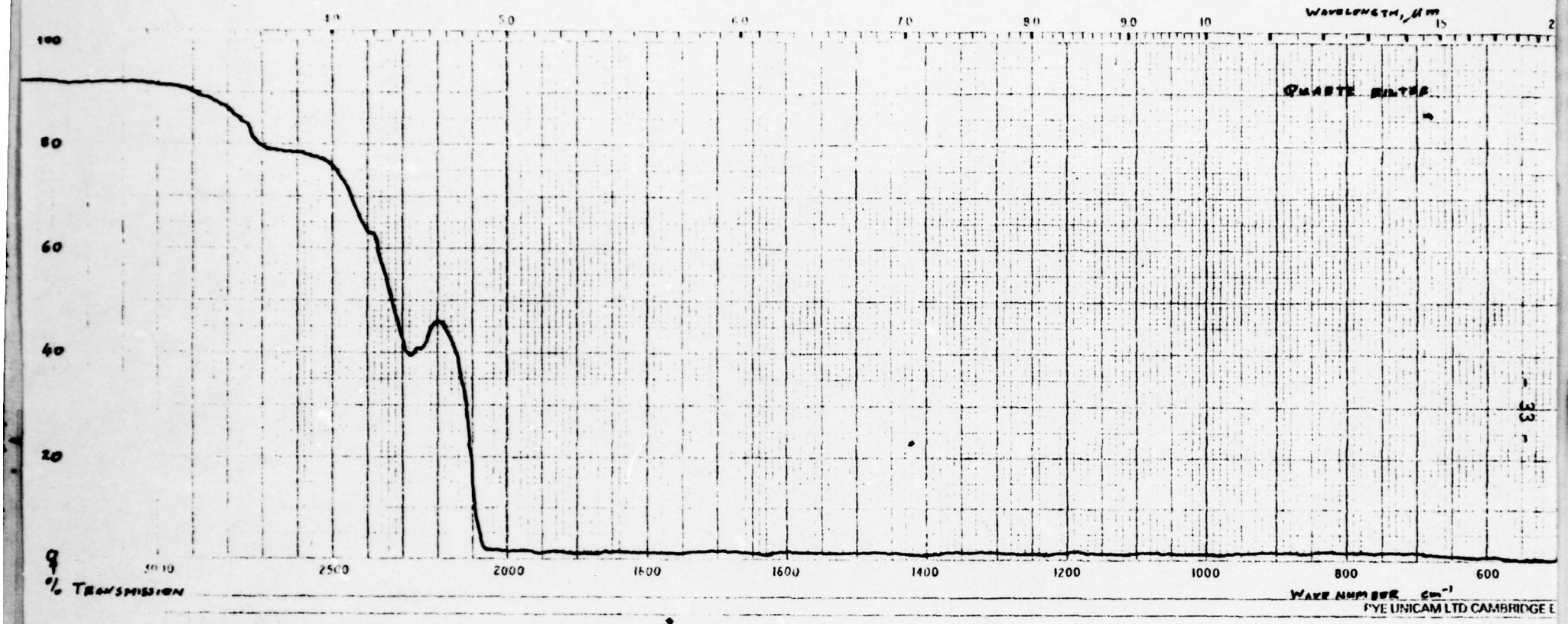

Figure 6: IR Absorption Spectrum for Quartz Filter.

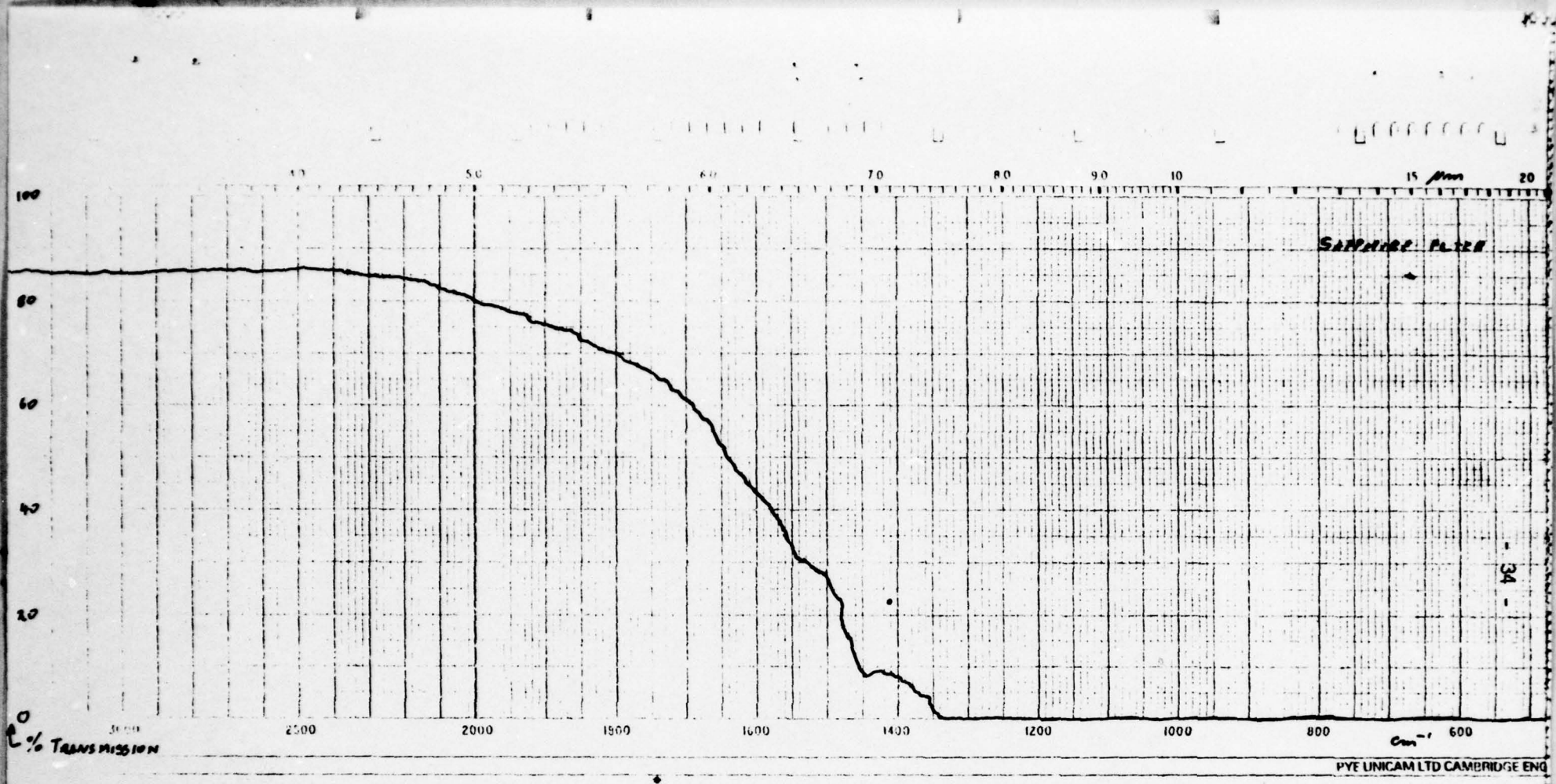

Figure 7: IR Absorption Spectrum for Sapphire Window.

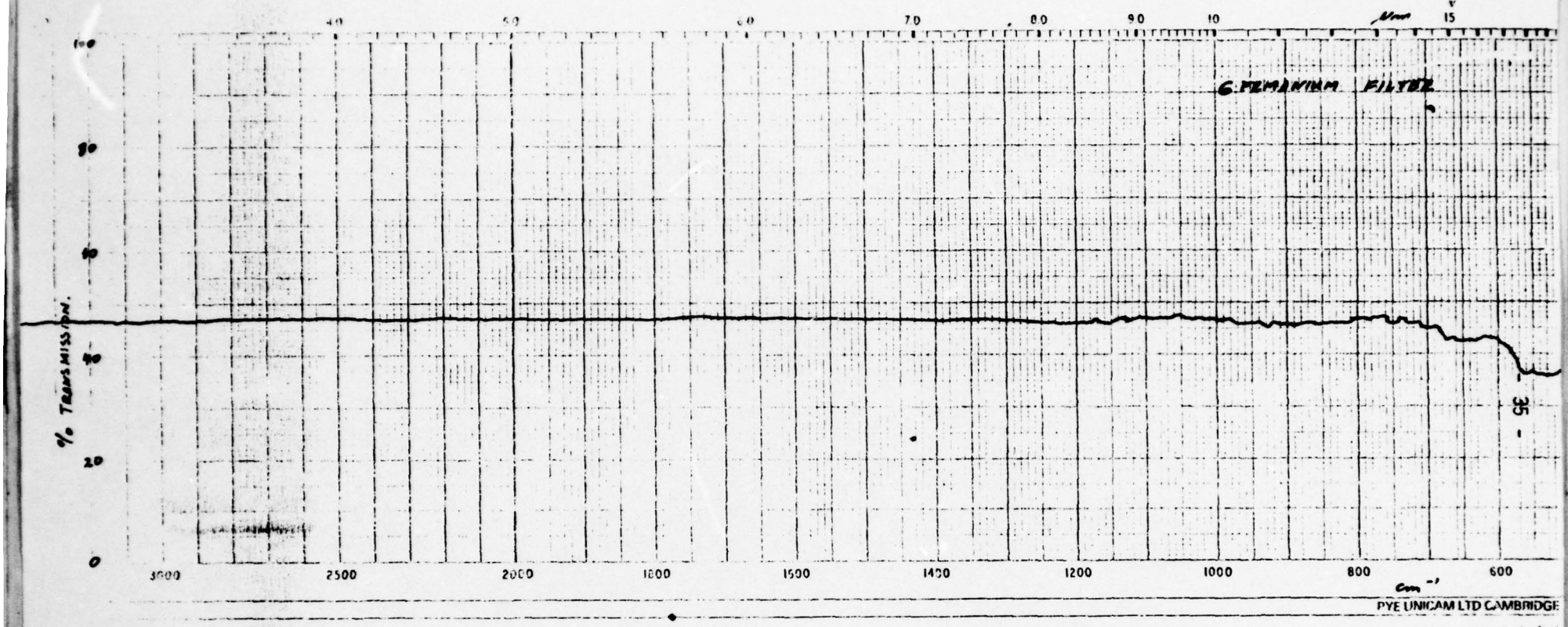

Figure 8: IR Absorption Spectrum for Germanium Window.

6.4 Flame Temperature Profile

A technique for measuring flame temperature profiles along the axis was developed. This was used to estimate radial heat loss from the flame and to serve as a comparison with the radiometer readings. Thermocouples (Pt/Pt-Rh) were mounted in a protecting ceramic sheath and traversed from the downstream end of the combustion tube. The thermocouples were calibrated at the tin m.p.

Care was taken to ensure that the thermocouples gave reliable flame temperatures. It was recognised that radiation from the thermocouple beads and conduction along the leads could reduce their temperature significantly below that of the surrounding gas. Tests with varying size beads, (.5-3 mm dia.) both with and without radiation shields, showed that the least uncertainty in temperature measurement occurred with the smallest bead (.5 mm dia.) unshielded. The small diameter wire used (0.1 mm) made conduction losses negligible.

The results of the temperature profiles showed significant heat losses from the combustion tube (Figure 9).

6.5 Profile Results

Preliminary work was carried out using natural gas (CH_4) and air. Figures 10-11 show the total radiation intensity of the flame without particles using the early burner design. Profiles with particles were not reliable due to difficulties in maintaining a uniform solids feed rate during the scan.

Figure 10 shows the effect of changing O/F ratio on radiation intensity and position of maximum. The quartz window was used. The presence of carbon and delayed combustion are evident. The 6% rich flame developed instabilities.

Figure 11 shows the radiant intensity at stoichiometric O/F ratio for different windows - quartz, sapphire and germanium. These have not been corrected for relative window transmission. The peaks in these curves can be compared with the thermocouple profile.

Figures 12 and 13 show the I.R. absorption spectra of samples of pure CO and CO_2 obtained in our laboratories. These identify the infra-red bands of interest, namely:

CO	4.4 - 5.0 μm
CO_2	2.6 - 2.8, 4.1 - 4.5, 13.4 - 17 μm

6.6 Solids Sampling Probe

A solids sampling probe based on iso-kinetic principles has been constructed - see figures 4,5. The system has yet to be trialed, pending modification to the solids feeder/burner assembly.

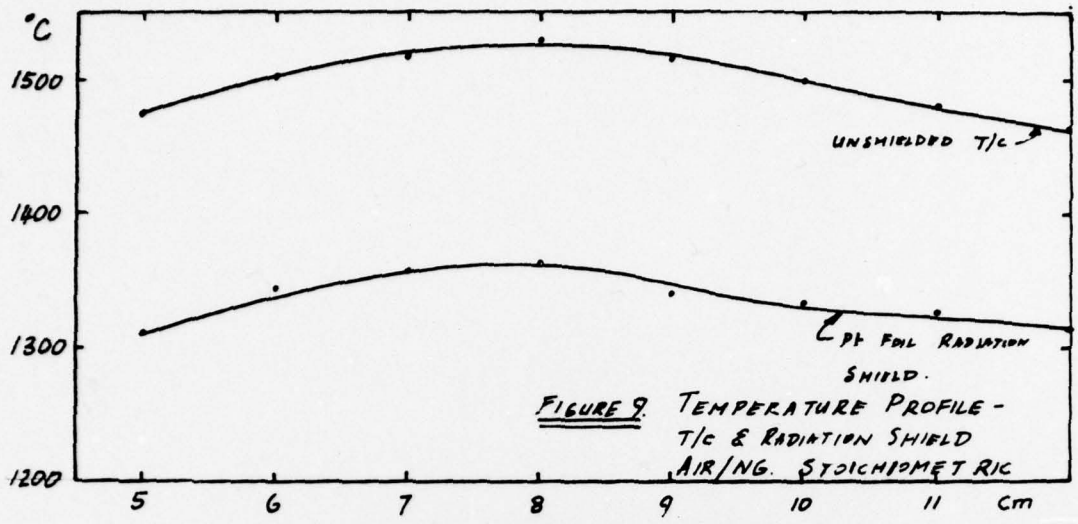

FIGURE 9. TEMPERATURE PROFILE - T/C & RADIATION SHIELD AIR/NG. STOICHIOMETRIC

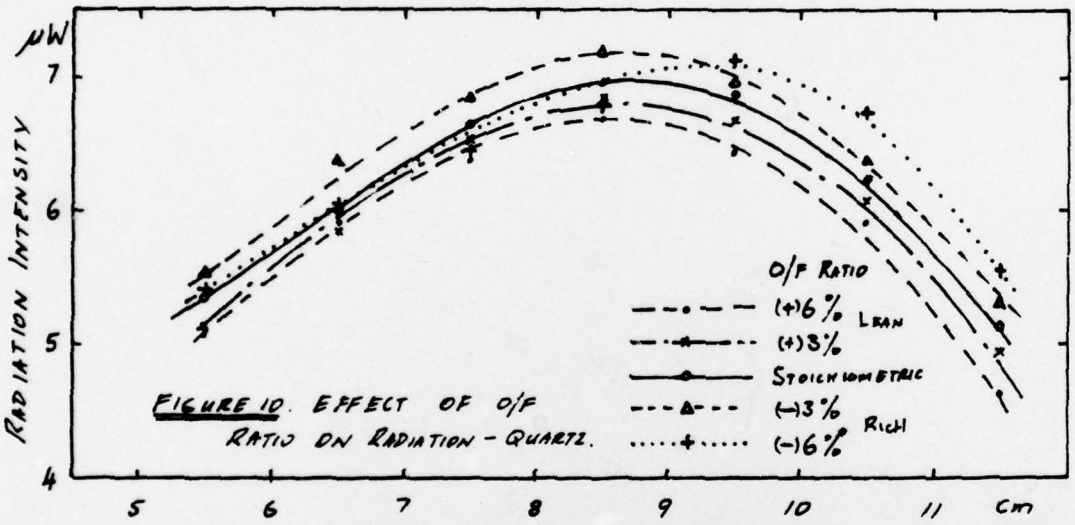

FIGURE 10. EFFECT OF O/F RATIO ON RADIATION - QUARTZ.

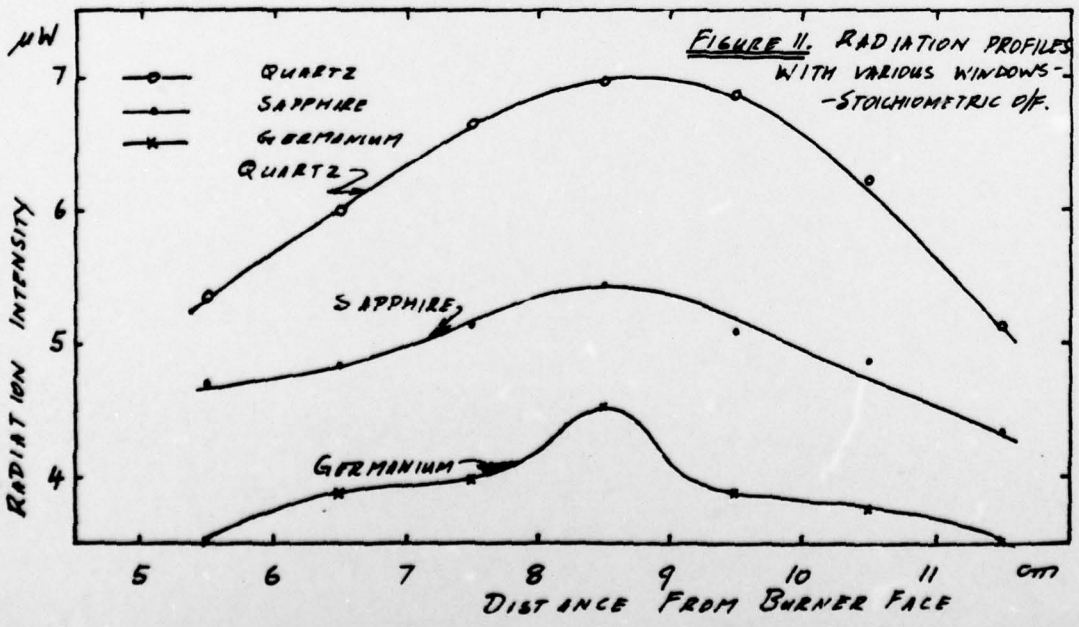

FIGURE 11. RADIATION PROFILES WITH VARIOUS WINDOWS - STOICHIOMETRIC O/F.

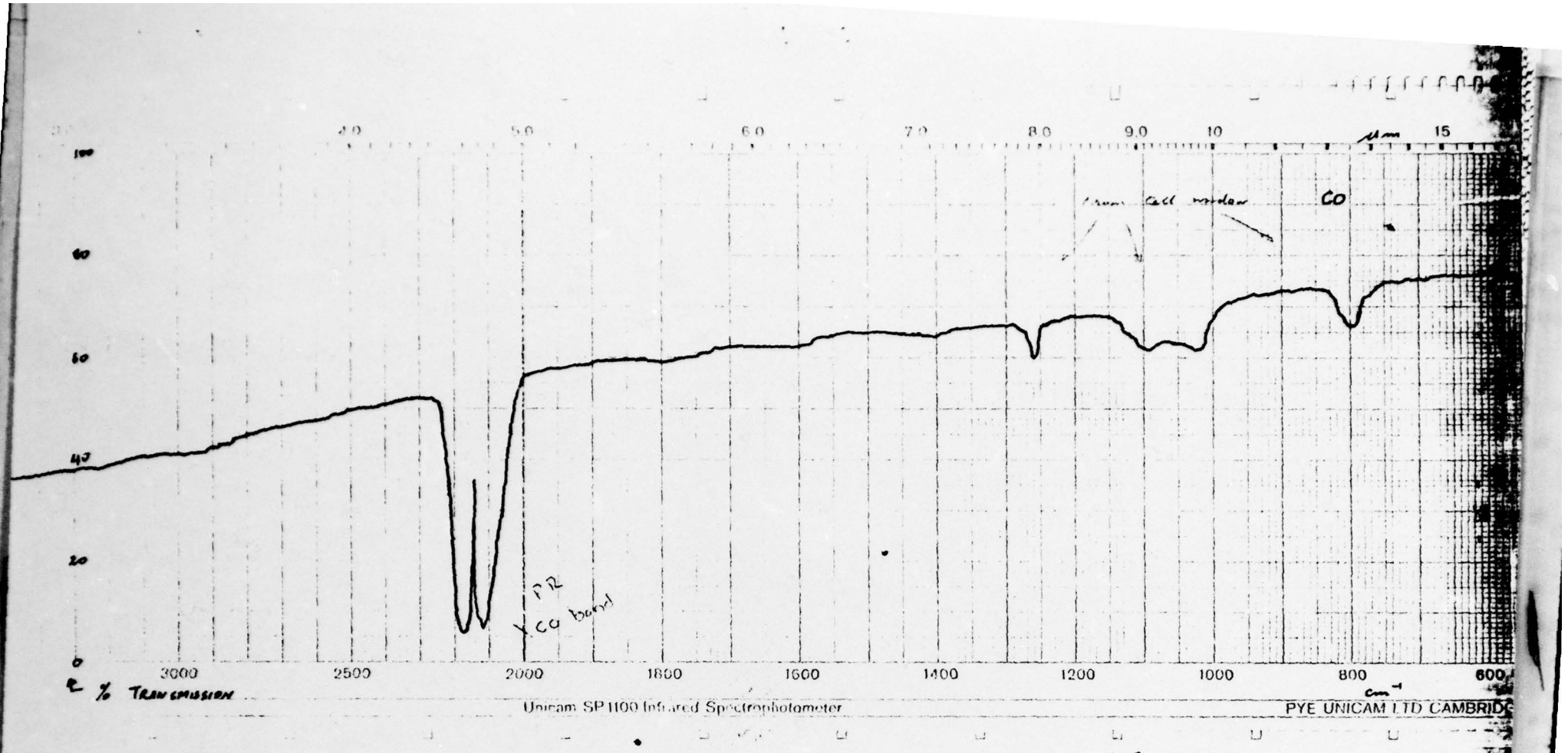

Figure 12: IR Absorption Spectrum for CO (1 atm), 10 cm path length. (Spurious peaks due to imperfections in sample cell windows.)

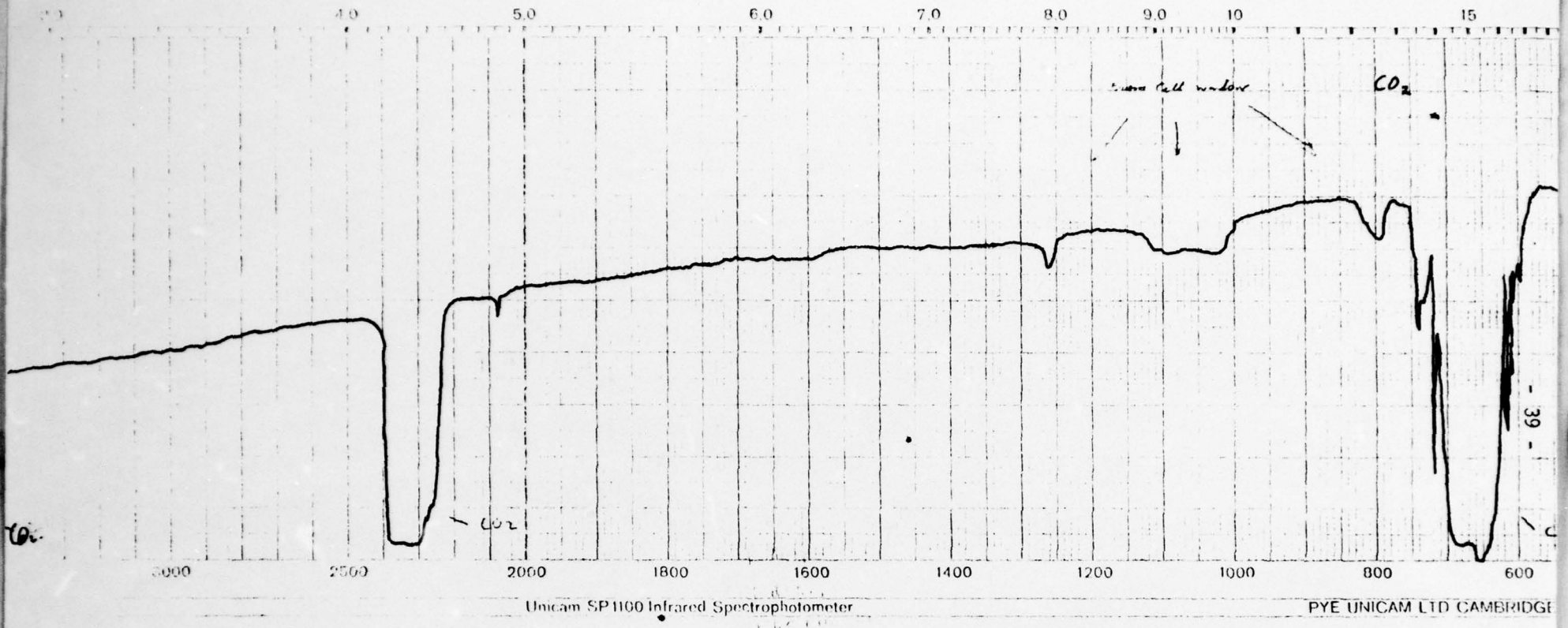

Figure 13: IR Absorption Spectrum for CO_2 (1 atm), 10 cm path length. (Spurious peaks indicated due to cell windows.)

7.0 SUMMARY

This report covers the work carried out during the period July 81 - June 82 on the project "Infra-red Characteristics of Gas Plumes". It contains a review of the available open literature and identifies areas where existing rocket exhaust plume models are deficient. Deficiencies were identified in modeling the turbulent structure of hot gas plumes particularly with the turbulent diffusion effects. Problems exist in estimating the spatial distribution of species and their concentration - due to lack of data on the kinetics of radical formation and combination especially in the presence of cationic modifiers such as K, Sn. The problem of particulate emissions both from liquid fueled motors (c) and metallized solid fuels (typically Al_2O_3) has not been solved adequately. Lack of optical parameters for some condensed species has hindered work in this area however the data for Al_2O_3 spheres is quite extensive.

An experimental rig has been designed, built and instrumented. Preliminary work has established its operability. Problems in burner design and particle addition have largely been solved. A system of solids sampling of the high temperature gas has not been fully tried-out pending improvements to the particle feeder.

This study should be continued to obtain data on particle addition to the flame, and the influence of particle size. Work on particle agglomeration/attrition in flames is warranted.

8.0 BIBLIOGRAPHY

The following bibliography lists all literature consulted in preparing the review. It includes material not specifically mentioned in this report. Copies of these references are held on file for all but a few cases such as texts, or where the material is held locally in the S.A.I.T. or Barr-Smith Libraries.

FILE NO.	AUTHOR(S)	CITATION	NTIS NO.
A 754/67	ARNOLD, G.D.	Developments in the Use of Oxy./Gas Burners, Journ. Inst. Fuel, March 1967, pp. 117-121.	
B 168/66	BAKER, D.J.	Stimulation of Optical Emissions in Atmospheric Gases. Utah State Univ., Logan. Electro-dynamics Labs. AF 19 (628) 251. AFCRL670058. 30th December, 1966.	AD 651 017
B 283/71	BARTLE, E.R. MECKSTROTH, E.A. KAYE, S.	Development of HCl and HF Detection System, Report No. AFRPL-TR-71-59, June 1971.	AD 884 193
B 565/75	BETTS, R.E.	Ignition Techniques for Studying Rocket Signature Effects ..... Army Missile Research Dev. & Eng. Lab. F/G 21/8 August, 1975. RK-76-4.	AD A016 876
B 674/73	BOGGS, T.L. ZURN, D.E.	Ammonium Perchlorate Combustion: Effects of ....., Combustion Science and Technology, Vol. 7, pp. 177-183.	
B 792/68	BOYNTON, F.P. LUDWIG, C.B. THOMSON, A.	Spectral Emissivity of Carbon Particle Clouds in Rocket Exhausts, AIAA Journ., 6 (5) pp. 865-871, May 1968.	
B 816/78	BRANCH, M.C.	Sampling from High Temperature Particle Laden Flows. Report SAND-78-8253 Sandin Labs., Albuquerque, N.M., July 1978.	
B 959/52	BURKET, S.C. MOE, G. NICHOLSON, J.L.	Chemical Kinetics Phenomena in Rocket Engines. Aerojet Eng. Corp., June 1952. WADC-TR-52-108.	AD A076 053
B 919/77	BUCHELE, D.R.	Computer Program for Calculation of a Gas Temperature Profile by Infrared Emission: Absorption Spectroscopy. NASA-TM-73848, Dec. 1977.	N 78 15043
C 552/80	CHOUDHURY, P.R.	Scaling and Performance of Dump Combustors with Transverse Gas Jets, AIAA Journ. 18 (4) pp. 450-454, April 1980.	
C 572/75	CILIBERTI, D.F. LANCASTER, B.W.	Modified "Harvard" Dry Dust Disperser, Rev. Sci. Inst. 46 (7) pp. 929-930, July 1975.	
C 678/71	COHEN NIR, E.	Combustion of Powered Metals in Contact with a Solid Oxidizer, Symp. on Combustion 13th, 1971, p. 1019.	
D 269/78	DAWBARN, R.	Aluminium Oxide Particles Produced by Solid Rocket Motors, Proc. USAF/NASA International Spacecraft Contamination Conf., Ed. J.M. Jemiola, AFML-TR-78-190, NASA-CP-2039.	AD A070 386

FILE NO.	AUTHOR(S)	CITATION	NTIS NO.
D 592/79	DIONNE, G.F. LITUAK, M.M. WEISS, J.A.	Detectability of Cold Rocket Plumes. MIT, Lexington Lincoln Lab., October 1979, TN-1979-48, ESD-TR-79-264.	AD A081 858/3
D 592/80	DIONNE, G.F. FITZGERALD, J.F. CHANG, T.S. LITUAK, M.M. FETTERMAN, H.R.	Radiometric Observations of the 752.033-GHz Rotational Absorption Line of H_2O from a laboratory Jet. J. of Infrared and Millimeter Waves, Vol. 1 No. 4, 1980, p. 582.	
D 632/67	DOBBINS, R.A. STRAND, L.D.	Recent Measurements at APL of Particle Size of Aluminium Oxide from Small Rocket Motors. NASA-CR-95688 June 15th, 1967.	N 68 29036
D 747/77	DOWLING, J.M. RANDALL, C.M.	Infrared Emissivities of Particles OFC, MgO, Al Al_2O_3, ZrO_2 at Elevated Temps. Final Report. 30th April, 1977. Chemistry & Physics Lab., The Aerospace Corp., ElSegrendo, Calif. TR-0077 (2641)-1, AFRPL-TR-77-14.	AD A042 144
D 749/74	DOWNIE, J.M. HOGGARTH, M.L.	A Review of Industrial and Commercial Gas Burner Developments, J. Inst. Fuel., June 1974 pp. 125-129.	
E 16/75	EBEOGLU, D.B. MARTIN, C.W.	Experimental Verification of Infrared Plume Predictions for Rocket Engines. AIAA Paper, No. 75-1231.	
E 16/74 /A	EBEOGLU, D.B. MARTIN, C.W.	The Infra Red Signature of Pyrophorics. AFATL-TR-74-92, May 1974.	AD 921 319
E 16/74 /B	EBEOGLU, D.B.	Fundamental Parameters Affecting Plume Infrared Radiation. AFATL-TR-74-84, April 1974.	AD 921 318
E 16/74 /C	EBEOGLU, D.B. HARWELL, K.E.	The Effect of Exit Velocity on the Infrared Radiation Intensity ..... AFATL-TR-74-10, Jan. 1974.	AD 918 420
E 27/74	EERKENS, J.W.	Rocket Radiation Handbook Vol. 1 Rocket "Radiation Phenomenology and Theory", June 1974, Garrett No. 74-9903-Vol-1 Airesearch MFG Co., LA, Calif.	AD A042 640
E 36/72	EISEL, J.L.	Combustion of NH_4ClO_4 - Polyurethane Propellants. AIAA Journal, Vol. 10, No. 12, p. 1655.	
F 394/65	FERRISO, C.C. LUDWIG, C.B. ACTON, L.	Spectral Emissivity Measurements of the 4.2 μ CO_2 Band between 2650 and 3000°K. August 1965, GD/C-DBE65-017, Space Sciences Lab.	AD 620 851
F 394/64 /A	FERRISO, C.C. LUDWIG, C.B.	High Temperature Spectral Emissivities of H_2O - CO_2 Mixtures in the 2.7 μ Region Applied Optics, Vol. 3, No. 12, 1964, p. 1435.	
F 394/64 /B	FERRISO, C.C.	Spectral Emissivities and Integrated Intensities of the 2.7 μ CO_2 Band between 1200 and 1800 K, J. Opt. Soc. Am. 54, p. 657, 1964.	
F 394/62	FERRISO, C.C.	High-Temp. Spectral Absorption of the 4.3-micron CO_2 band. J. Chem. Phys. 37 (9) 1955, (Nov. 1962)	
F 565/72	FIVES, E.A.	A Flow Tube Facility for Molecular Spectroscopy. TR-0172(2220-20)-4, SAMSO-TR-72-6, January 1972.	

FILE NO.	AUTHOR(S)	CITATION	NTIS NO.
F 855/79	FREEMAN, G.N. LUDWIG, C.B. MALKMUS, W. REED, R.	Development and Validation of Standardised Infrared Radiation Model (SIRRM). Gas/Particle Radiation Transfer Model. AFRPL-TR-79-55, October 1979.	AD A076 199
G 195/79	GANY, A. CAVENY, L.H. SUMMERFIELD, M.	Aluminized Solid Propellants Burning in a Rocket Motor Flow Field, AIAA Journal, Vol. 16, No. 7, pp. 736-739.	
G 369/63	GERKE, P.D. GALIGHER, L.L.	Wind Tunnel Studies of Rocket Engine Plume Infrared Radiation in Supersonic flow. Tech. Doc. Report No. AEDC-TR-62-224, January 1963. Propulsion Wind Tunnel Facility, ARO Inc., Arnold Engineering Dev. Cent., Airforce Systems Command, USAF.	AD 335 203
G 481/80	GILLILAND, T.M.	Jannaf Plume Technology Meeting (12th) U.S. Air Force Academy. December 1980, CPIA-PUB-332-Vol-1.	AD A096 988
G 615/79	GOIN, K.L. McCLURE, J.G.	System for Dispensing and Continuously Measuring the Flow of Solid Particles into a Hot High Pressure Gas Flow. Rev. Sci. Inst. 50 (2) pp. 236-240 (February, 1979).	
G 632/77	GOMBERG, R.I. KANTSIOS, A.G. ROSENSTEEL, F.J.	Some Physical and Thermodynamic Properties of Rocket Exhaust Clouds Measured with Infrared Scanners. NASA-TP-1041, November 1977.	N 78 11520
G 895/76	GRYVNAK, D.A. BURCH, D.E.	Monitoring NO and CO in Aircraft Jet Exhaust by Gas Filter Correlation Technique. AFAPL-TR-75-101, January 1976.	AD A022 353
H 116/67	HABICHT, R.F.	The Effect of Aluminium on the Emission Spectra of Solid Propellants. U.S. Naval Postgrad. School M.Sc.(Phys.) Thesis, June 1967.	AD 820 948
H 343/78	HARWELL, K.E.	Refinement on Plume Modeling in the Infrared Spectral Region. Tenn. Univ. Space. Inst., Tullahoma, June 1978. DAAK40-77-C-0032.	
H 343/77	HARWELL, K.E.	Comparison of Theoretical and Experimental Infrared from a Rocket Exhaust. Progress in Astronautics & Aeronautics. Vol. 59, pp. 186-203.	
H 343/76 /A	HARWELL, K.E.	Infrared Radiation Characteristics of a Hot Gas Generator. AIAA Paper 76-143.	
H 343/76 /B	HARWELL, K.E.	Development of Theoretical Models and Description of Computer p...etc. Report DAAHOI-75-C-0121. September 1976,	AD A030 380
H 343/76 /C	HARWELL, FULLER, JACKSON, POSLAJKO	"Three Dimensional Laser Doppler Velocimeter Measurements of the Velocity Distribution in a Supersonic Jet Mixing with a Subsonic Outer Flow", AIAA Paper 26-24, January 1976.	
H 361/81	HATAMI, R.	Calculation of Combustion Instabilities of Enclosed Diffusion Flames. The Chem. Eng. Journ. 22(1981)1-14.	
H 889/68	HUFFAKER, R.M.	Current Research on Infrared Radiation from Rocket Exhaust. J. Quant. Spectrosc. Radiat. Transfer., Vol. 8, pp. 87-104.	

FILE NO.	AUTHOR(S)	CITATION	NTIS NO.
J 13/75	JACKSON, H.T. POSLAJKO, F. HARWELL, K.E.	Measurements of Infrared Radiation Characteristics of a Small Kerosene/Oxygen Hot Gas Generator, U.S. Army Missile Research, Dev. and Eng. Lab. TR-RE-76-1, July 1975.	AD A017 296
J 54/75	JENSEN, D.E. WILSON, A.S.	Prediction of Rocket Exhaust Flame Properties Combustion and Flame, Vol. 25, pp. 43-55.	
J 54/73	JENSEN, D.E. WILSON, A.S.	Rapid Computation of Physical and Chemical Structures of Rocket Exhaust Flames.	
J 54/71	JENSEN, D.E. JONES, G.A.	Flame Photometric Determination of the Standard Enthalpies of Formation of $Al(OH)_2$ and AlO. RPE-TR-71/9, 1971.	
K 62/79	KISHORE, K.	Models of Composite Solid Propellants, AIAA Vol. 17 No. 11, pp. 1216-1224.	
K 64/67	KLEIN, L. PENZIAS, G.J.	Spectral Radiances of Model Rocket Exhaust Gases at Simulated Altitutde Measured with a Rapid-Scanning Spectrometer, AIAA Journ. Vol. 5, No. 9, p. 1690.	
K 66/75	KOLB, C.E. CAMAC, M. SUBBARAO, R.B. ANDERSON, J.B.	Experimental Studies of the Collisional Excitation of Infrared ..... ARI-RR-55, AFRPL-TR-75-2, Feb. 1975.	AD A006 237
K 91/77	KRAKOW, B. KIECH, E.L. McADOO, H.A.	Isolated CO Lines for Use in Combustion Gas Diagnostics. September 1977, AEDC-TR-77-11.	AD A044 053
L 425/68	LAWTON, J. MORRISON, M. SCHELLER, K.	Radiative Transfer from an Inhomogeneous Non Scattering Gas in the ..... July, 1968, Proj. AF-7023.	AD 675 996
L 629/81	LESINSKI, J. MIZERA-LESINSKA, B., FANTON, J. C., BOULDS, M.I	Laser-Doppler Anemometry Measurements in Gas Solid Flows, AICHE Journ. 27 (3) pp. 358-364, May 1981.	
L 733/77	LIMBAUGH, C.C.	An Uncertainty Propagations Analysis for an Infrared Band Model. AEDC-TR-76-155, April 1977.	AD A038 063
L 747/75	LINDQUIST, G.H. ARNOLD, C.B. SPELLICY, R.L.	Atmospheric Absorption Applied to Plume Emission. ERIM-102700-20-F, AFRPL-TR-75-30, August 1975.	AD A015 075
L 791/69	LLINAS, J. McCAA, D.J.	Spectral Radiance of Model Rocket Exhaust Plumes at High Altitudes, Paper 68-767, AIAA 3rd Thermo-Physics Conf., LA, Calif. June 1968, NAS 8-2007.	
L 948/78	LUDWIG, C.B. MALKMUS, W. REARDON, J.E. THOMSON, J.A.L.	Handbook of Infrared Radiation from Cumbustion Gases. NASA SP-3080, 1973.	
M 121/68	McCAA, D.J.	Spectral Radiance Measurements of Exhaust Plumes from Scale Model Rocket Engines, Applied Optics, Vol. 7, No. 5, p. 899.	
M 149/75	McHALE, E.T.	"Supression of Missile Plume Infrared Signature". Atlantic Research Corp. Submitted to Naval Ordinance Station Under Contract No. N00174-74-C-0270, ARC Ref. No. 47-5626, 20th October, 1975.	
M 359/69	MARRIOTT, R.	Progress Report, June 15-Dec. 15th, 1969, Wayne State Uni. Detroit, Mich. Dec. 1969, F04701-69-C-0230.	AD 697 967

FILE NO.	AUTHOR(S)	CITATION	NTIS NO.
M 379/74	MARTIN, C.W. ASKEW, R.E. EBEOGLU, D.B.	Operation of an Infrared Thermal Scanner for Plume Measurements. December 1974, AFATL-TR-74-204.	AD B002 928
M 361/73	MARRONE, P.V.	Plume Interference Assessment and Mitigation. Report No. DAMC60-69-C-0035 CALSPAN-KC-5134-A-6.	AD 913 714
M 862/64	MORIZUMI, S.J. CARPENTER, H.J.	Thermal Radiation from the Exhaust Plume of an Aluminized Composite Propellant Rocket. J. Spacecraft, 1, (5), 501 (1964).	
N 163/82	NAKAMLIRA, Y. UCHIDA, S.	Numerical Solutions of the Navier-Stokes Equations for Axisymmetric Weak Swirling Flows in a Pipe. Jap. Soc. for Aeronautical and Space Sciences, Trans. 24 (66) pp. 222-226, February 1982.	
N 632/75	NICKERSON, G.R.	Nonequilibrium Radiation Model for Exhaust Plumes. March 1975, AFRPL-TR-74-74.	AD A007 795
P 142/79	PAI VERNEKER	Combustion of Ammonium Perchlorate - Aluminium Mixtures. J. Spacecraft 16, (6) 436 (Nov.-Dec. 1979).	
P 439/77	PERGAMENT, H.S. FISHBURNE, E.S.	Properties of Large Turbulent Hydrogen/Air Diffusion Flames. Oct. 1977.	AD A052 781
P 439/76	PERGAMENT, H.S. THORPE, R.D.	Chemical Kinetic/Gas Dynamic/Particle Interactions in Rocket Nozzle and Exhaust Plume Flows, Sept. 1976. Aerochem.-TP-345, AFOSR-TR-76-1143.	AD A032 675
P 439/71	PERGAMENT, H.S. JENSEN, D.E.	Influence of Chemical Kinetic and Turbulent Transport Coefficient on Afterburning Rocket Plumes. J. Spacecraft and Rockets, 8, (6) 643.	
P 439/67	PERGAMENT, H.S. & OTHERS	Thermal and Chemi-Ionization Processes in Afterburning Rocket Exhausts. 11th Symposium (International) on Combustion, Vol. 11, 1967, pp. 597-611	
P 466/78	PERSKY, M.J.	0.1 Wavenumber Spectral Measurements in the Region from 2050 to 2410 cm^{-1}. Block Engineering Inc. Cambridge, Mass. Report No. N60530-78-G0272 BEI-78-761, December 1978.	AD A073 704
P 715/64	PLASS, G.N.	MIE Scattering and Absorption Cross Sections for Al_2O_3, MgO. App. Opt. 3 (7) pp. 867-872, July 1964.	
P 957/75	PRINCETON UNIVERSITY	Compilation of Abstracts - 1975 AFOSR Contractors Meeting on Combustion Kinetics, Sept. 1975, Princeton University, N.J. School of Aerospace and Mechanical Engineering, AFOSR-TR-75-1448, AF-AFOSR-2604-74.	AD A015 713
R 288/70	REARDON, J.E.	Prediction of Radiation from Rocket Exhaust Gases. Paper No. 70-841, AIAA 5th Thermophysics Conf., LA, Calif., June 1970.	
R 288/73	REARDON, J.E.	A Computer Program for the Prediction of Radiation from Rocket Exhaust Plumes. Vol. 1, May 1973, RTR-013-1-Vol-1, DAAHOI-73-C-0252.	AD A037 385
R 288/74	REARDON, J.E. McKAY, G.B. SOMERS, R.E.	Plume Infrared Radiation Characteristics. Mar. 74 RTR-013-2, DAAHOI-73-C-0252.	AD 776 407

FILE NO.	AUTHOR(S)	CITATION	NTIS NO.
R 325/78	REED, R.A.	Fourier Transform Infrared Spectroscopy: Demonstration of Measurement Capabilities. Jan. 1978, Grumman Aerospace RM-648.	AD A051 444
R 547/80	RIDOUT, J.M. WEBB, B.C.	Dual Waveband Infrared Scanning Radiometer for use with Rocket Motor Plumes, SPIE Vol. 234, New Developments and Applications in Optical Radiation Measurements (Sira) 1980, pp.32-39.	
R 554/73 /A	RIEGER, J.J. BAUM, H.R. KOLB, C.B. TAIT, K.S. BERMELES, A.E.	Rocket Plume Radiation due to Interactions with the Atmosphere, Vol. 1, Far Field Plume Radiation Model, July 1973, Report No. Calspan Corp. ARI-RN-20VI.	AD 913 820
R 554/73 /B	RIEGER, T.J. WORSTER, B.W. MORAN, J.P.	Rocket Plume Radiation due to Interactions with the Atmosphere, Vol. 2, Plume Radiation Predictions for Athena H second and third stage boosters, July 1973, Report No. ARI-RN-20VS, Calspan Corp.	AD 913 821
R 554/75	RIEGER, T.J. BAUM, H.R.	Atmospheric Interaction Radiation from High Altitude Rocket Exhausts. J. Quant. Spectrosc. Radiat. Transfer. Vol. 15, 1117-1124 (1975).	
R 554/79	RIEGER, T.J.	On the Emissivity of Aluminium/Aluminium Composite Particles, J. Spacecraft, Vol. 16, No. 6, pp. 438-9.	
R 737/77	ROH, W.B.	Coherent Anti-Stokes Raman Scattering of Molecular Gases. Aug. 1977, SRL-6856, AFAPL-TR-77-47.	AD A050 156
R 847/76	ROTHSCHILD, W.J. MARTIN, C.W.	Experimental Results for Hydrocarbon Exhaust Infrared Model ..... July 1976, AFATL-TR-76-74.	AD A037 252
R 871/79	ROUX, J.A. & OTHERS	Optical Properties of Bipropellant Exhaust Constituents Condensed at 77K, J. Spacecraft, Vol. 16, No. 6, pp. 373-381.	
R 871/78	ROUX, J.A.	IR Scanning Camera Measurements of an Exhaust Plume from an Axisymmetric Nozzle Afterbody Model at Transonic Mach Numbers, SPIE Vol. 156, (iv) 1978.	
R 916/81	RUDMAN, S.	Multi-Nozzle Plume Flow Fields, (1981) Grumman Aerospace RE-618, AFOSR-TR-81-0307.	AD A097 244
S 496/66	SEVBOLD, J.	Turbulent Mixing of a Two Dimensional Free Jet. Hughes Aricraft Co., Sept. 1966, FLD/GP 20/4.	AD 809 324
S 592/65	SIMMONS, F.S. ARNOLD, C.B. SMITH, D.H.	Studies of Infrared Radiative Transfer in Hot Gases. I. "Special Absorptance Measurements in The 2.7 μ H_2O Bands. Aug. 1965, Inst. Sci. Tech., Univ. Mich.	AD 468 750
S 949/77	SUKANEK, P.C. & OTHERS	A Band Model for Calculating Radiance and Transmission of Water Vapour and CO_2, Progress in Astronautics and Aeronautics, Vol. 59, pp. 204-222.	
T 521/77	THORPE, R.D. & OTHERS	A Comparison of Calculated and Measured Rocket Plume Infrared Radiation, Progress in Astronautics and Aeronautics, Vol. 59, pp. 177-185.	
T 923/78	TULLY, F.P. RAVISHANKARA, A.R.	The Kinetics and Spectroscopy of Aircraft and Rocket Plume Constituents. Georgia Inst. Tech., July 1978. AFOSR-TR-78-1280.	AD A059 809

FILE NO.	AUTHOR(S)	CITATION	NTIS NO.
V 228/76	VANDERBILT, D.	A Model for Emission and Scattering of Infrared Radiation from Inhomogeneous Combustion Gases and Particles. June 1976, RM-621 Grumman Aerospace.	AD A027 576
V 643/66	VICTOR, A.C. BUECHER, R.W.	An Analytical Approach to the Turbulent Mixing of Coaxial Jets. October 1966, Navweps. 9057.	AD 646 319
W 339/77	WATSON, G.H. LEE, A.L.	Thermal Radiation Model for Solid Booster Plumes, J. Spacecraft and Rockets, Vol. 14, 1977, pp. 641-647.	
W 578/75	WHITSON, M.E.	Handbook of the Infrared Optical Properties of Al_2O_3, C, MgO, ZrO_2, Vol. 1, 4th June, 1975, Chemistry & Physics Lab., Aerospace Corp., SAMSO-TR-75-131 - Vol. 1, TR-0075(5548) - 2 - Vol. 1.	AD A013 722
W 721/74	WILLIAMS, A. HORNE, W.	The Use of Oxy-Fuel Combustion in Industrial Heating Processes. Rev. Roum. Sci. Techn. - Electro. Techn. et. Energ. 19 (4), pp. 649-656.	
W 756/79	WILTON, M.E.	Advanced Infrared Signature Prediction Program. Vol. III "Analysis". November 1979. General Elec. Co. R78AE6314.	AD A078 436
W 931/75	WORSTER, B.W.	Particulate Infrared Radiation in Aluminized Solid-Fuel Rocket Plumes, J. Spacecraft, Vol. 11, No. 4.	
W 958/73	WRUBEL, J.A.	Study of Dual-Channel Infrared Spectroradiometer Systems. March 1973. NASA-CR-124207.	N 73-21387
Y 76/78	YOUNG, S.J.	Inversion of Plume Radiance and Absorptance Data for Temp. September 1978. TR-0078(3623)-2, SAMSO-TR-79-30.	AD A068 437
Y 76/75	YOUNG, S.J.	Band Model Calculation of Atmospheric Transmittance for Hot Gas. July, 1975, TR-0076(6970)-5, SAMSO-TR-75-212.	AD A013 719
Z 16/79	ZACHOR, A.S. HOLZER, J.A. SMITH, F.G.	I.R. Signature Study. Honeywell Electro-optics, February 1979, 7812-8, AFAL-TR-79-1012.	AD A072 374
Z 41	ZEBEL, G.	Some Problems in the Sampling of Aerosols, Chapter 8, pp. 167-185.	
Z 81/66	ZIRKIND, R.	Radiation from Rocket-Exhaust Plumes. Polytech. Inst. Brooklyn, August 1966. RPIBAL 984.	AD 641 612

9.0 NOMENCLATURE

A	=	throat area
a_1, a_2	=	Universal empirical constants
b_D	=	Doppler broadened line half width
Cp	=	specific heat at constant pressure
d	=	distance (cm) between adjacent spectral lines
E	=	Internal energy
K	=	mixing rate factor
L	=	local length scale
M	=	Mach number
$\dot{M}$	=	mass flow rate
m	=	molecular weight
P_c	=	chamber pressure
P_e	=	exit pressure
Pr_k	=	turbulent Prandtl number
$P(S)$	=	probability function
p	=	pressure
$\vec{q}$	=	heat flux vector
r	=	radius
s	=	line intensity
T	=	temperature (K)
t	=	time
U	=	optical depth
U_s	=	typical velocity difference
u	=	x velocity component
$\vec{V}$	=	velocity vector
V	=	specific heat ratio
v	=	y velocity component
X	=	length vector

α = Mie parameter ($= 2\pi r/\lambda$)

$\bar{\varepsilon}$ = mean emissivity of spectral band

ε_t = turbulent diffusivity

γ = line half width

ω = wave number

ρ = density

$\underline{\underline{\tau}}$ = shear stress tensor

λ = wavelength

μ = dynamic viscosity

Dear Dr Stevens

I would very much appreciate a copy, if available of your article

IR Characteristics of Gas Plumes

which appeared in

Thank you for this courtesy.

Yours Sincerely,

R. GOLDSACK 70851

Senior Scientist - Air

Copies to Dr. R Goldsack.
State Pollution Control Commission
Box 4036, GPO Syd.
NSW 2001

27 Apr 84.

DIST: Authors - (2) 1.0
DRCS - 2 2.0

Copy 1 of 4

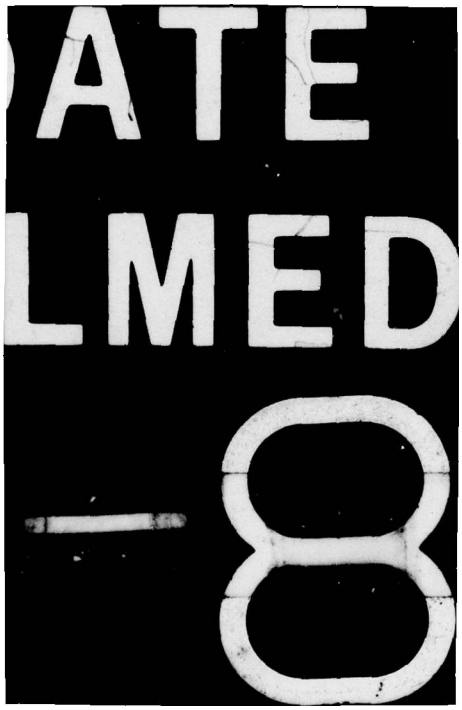
ATE
LMED
8